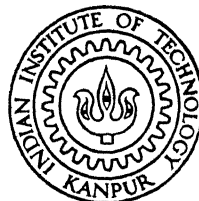


# TEMPERED MARTENSITE EMBRITTLEMENT IN AISI 4135 STEEL

*by*

SHRIPAD RAMCHANDRA PONKSHE



ME  
1990  
M  
PON  
TEM

DEPARTMENT OF METALLURGICAL ENGINEERING  
INDIAN INSTITUTE OF TECHNOLOGY KANPUR  
FEBRUARY, 1990

# **TEMPERED MARTENSITE EMBRITTLEMENT IN AISI 4135 STEEL.**

*A thesis submitted  
in partial fulfilment of the requirements  
for the degree of*

**MASTER OF TECHNOLOGY**

**By**

**SHRIPAD R. PONKSHE**

**to the**

**DEPARTMENT OF METALLURGICAL ENGINEERING  
INDIAN INSTITUTE OF TECHNOLOGY, KANPUR**

**FEBRUARY, 1990.**

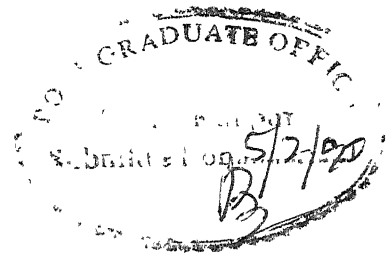
ME-1990-M-PON-TEM

109078

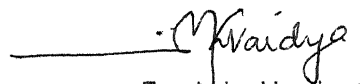
CE 109078

Acc. No. 109078

CERTIFICATE



It is certified that this work entitled "TEMPERED MARTENSITE  
EMBRITTLEMENT IN AISI 4135 STEEL" has been carried out by Mr. Shripad  
Ramchandra Ponkshe under my supervision and the same has not been  
submitted elsewhere for a degree.

  
(Dr. M.L. Vaidya)

Professor and Head

Deptt. of Metallurgical Engg.

I.I.T. Kanpur.



### ACKNOWLEDGEMENT

I take this opportunity to express my profound gratitude and appreciation to Dr. M.L. Vaidya for his inspiring and valuable guidance and persistent encouragement provided to me at all stages of the present work. It was indeed a pleasure to work with him.

I am also indebted to the staff of Advanced Centre for Material Science, IIT Kanpur for allowing me to use the facility of SEM and providing all other necessary help in microscopy. Thanks are also due to Mr. B.K. Jain, Mr. H.C. Srivastava, Mr. K.P. Mukherjee and other staff of Metallurgical Engineering Department for their help and cooperation.

I also thank my friends, especially Mr. M.V. Joshi and Mr. M.G. Bhargava who provided me the necessary inspiration and encouragement throughout my stay in IIT K.

Last but not the least thanks are due to all my batchmates who made my stay at this campus pleasurable and memorable one.

S.R. Ponkshe  
(S.R. Ponkshe)

## CONTENTS

### ABSTRACT

PAGE NO

#### CHAPTER - I INTRODUCTION

1.1 Measure of TME	1
1.2 Technological Significance of TME	2
1.3 Parameters affecting TME	4
1.4 Objectives of Present Investigation	4

#### CHAPTER - II LITERATURE REVIEW

2.1 Effect of Alloying Elements	6
2.2 Impurity Content	10
2.3 Effect of Retained Austenite	13
2.4 Role of Carbides and Nitrides	18
2.5 Fracture Modes	22
2.6 Effect of Evaluation Methodology	27
2.7 The Testing Temperature and TME	30
2.8 Effect of Tempering Time	33
2.9 Mechanisms of TME	34

#### CHAPTER - III EXPERIMENTAL PROCEDURE

3.1 Material	39
3.2 Preparation of Test Specimens	39
3.3 Heat Treatment	42
3.4 Mechanical Testing	42
3.5 Scanning Electron Microscopy	
(a) Metallography	43
(b) Fractography	43

CHAPTER - IV	EXPERIMENTAL RESULTS AND OBSERVATIONS	
4.1	Variation of Hardness with Tempering Temperature	46
4.2	Impact Toughness Variation with Tempering Temperature	46
4.3	Variation of Plane-Strain Fracture Toughness ( $K_{Ic}$ ) with Tempering Temperature	47
4.4	Variation of Impact Toughness Values with Time at 350° C	48
4.5	Microstructural Study	
	(a) Variation of Tempering Temperature	49
	(b) Variation of Tempering Time	50
4.6	Fractographic Studies	
	(a) C/N Fracture Surfaces	51
	(b) $K_{Ic}$ Fracture Surfaces	51
CHAPTER V	DISCUSSION	64
CHAPTER VI	CONCLUSIONS	72
REFERENCES		74

## ABSTRACT

The Tempered Martensite Embrittlement has been studied in AISI 4135 steel by means of Charpy impact and fracture toughness test carried on specimens tempered in the entire range of tempering temperature (200° C to 550° C). The embrittlement in Charpy impact test has been shown by minimum in toughness at 350° C and it was shifted to 450° C in case of  $K_{IC}$  testing. Correlation of microstructural changes and Fracture initiation process in two different evaluation methods has been made. The mechanism for the T.M.E. in Charpy and  $K_{IC}$  testing has also been proposed for the present steel. The dependency on carbide morphology (ribbon shaped) in case of Charpy impact test and the inter particle (cementite) distance, along with number of microvoids produced in case of  $K_{IC}$  testing, are the proposed causes behind the T.M.E. phenomena. In addition to study on effect of testing methodology, effect of tempering time in T.M.E. region and prestraining has also been made.

-----

## INTRODUCTION

---

For many years it has been known that the high or ultra high strength grades of steels undergo an embrittlement during tempering. This is indicated by sudden drop in Charpy impact values in certain temperatures range of tempering. In spite of decrease in strength with tempering temperature, the occurrence of this embrittlement at lower temperature is known as "Tempered Martensite Embrittlement" (T.M.E.). This also has been known as 300° C or 500 F embrittlement in some earlier references as it usually occurs around this temperature. This embrittlement is not the classical intergranular as temper embrittlement due to impurity segregation &/or precipitation at the grain boundaries i.e. fracture is not necessarily intergranular and occur even in the carefully vacuum melted experimental steels wherein the impurity content is much lower than commercial steels. This T.M.E. phenomena doesn't tie to any specific temperature, composition or sequence of processing operations.

### 1.1 Measure Of T.M.E.:

The magnitude of minimum toughness value (CVN test) which is obtained during tempering cycle, indicates the degree of embrittlement. When the Charpy V notch impact toughness values are plotted against tempering temperature, the severity of embrittlement in quantitative terms can be considered by -

- 1.) The depth of trough i.e. difference between maximum toughness value before embrittlement and the minimum toughness value ( $\delta E$ ).

2 > The range of tempering temperature over which trough occurs

In general, higher the depth of trough &/or wider the range over which trough lies higher the severity of embrittlement is considered

A typical T. M. E trough commonly observed in low medium carbon steel is shown in fig 11 .

## 1.2 Technological Significance of T.M.E.:

It has been well established that the optimum property development of high strength low alloy steels can be achieved by quenching and tempering the steel components. The usual practise in such a heat treatment is oil quenching and tempering at such a value of temperature at which the best combination of toughness and strength will be obtained. With the increase in tempering temperature the strength decreases and toughness is expected to be increased. The role of T.M.E. becomes significant in designing such a critical tempering temperature at which necessary toughness is maintained along with strength. In order to escape from this embrittlement phenomena usually high temperature tempering procedures are adopted. In such a practice compared to low temperature of tempering two types of losses are encountered -

- 1.) Increase in fuel energy consumption and time needed for tempering operation, which can be considered as economical loss.
- 2.) Softening of matrix and therefore lowering of strength, which comes under mechanical property loss.

Thus it becomes necessary to analyze the basic cause or causes behind the interesting phenomena.

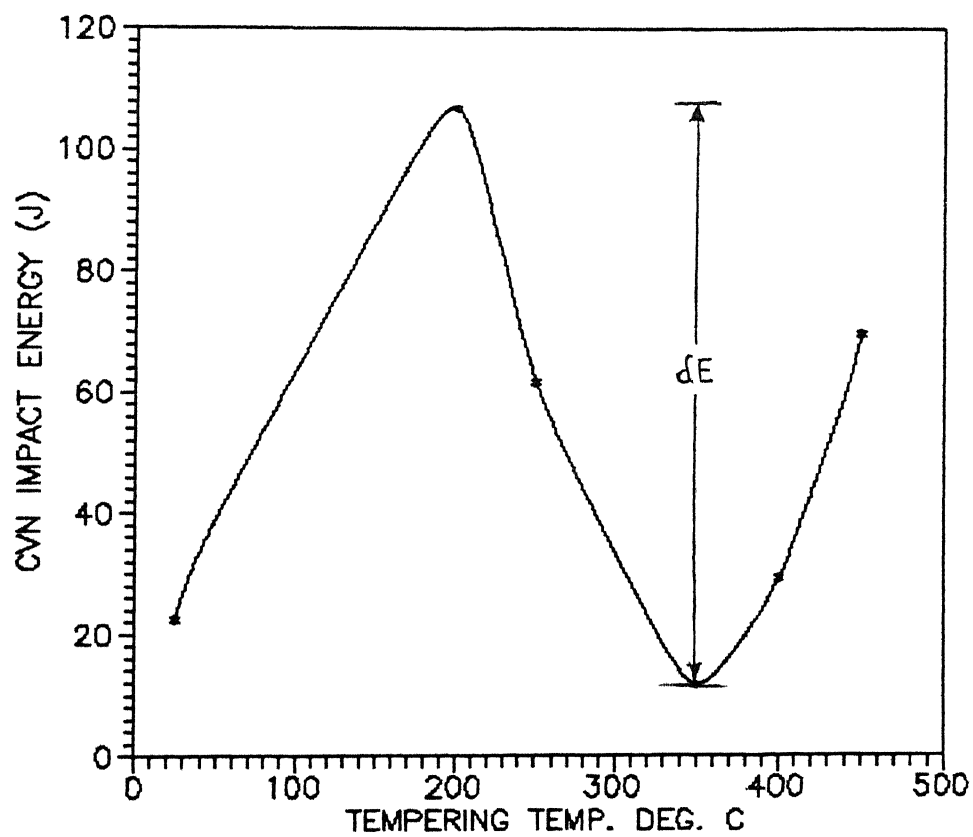


FIG.1-1 SHOWS TYPICAL T. M. E.  
TROUGH IN LOW ALLOY MEDIUM  
CARBON STEEL.

### 1.3 Parameters Affecting T.M.E.:

As the T.M.E. phenomena is related to toughness - microstructure correlation, it is very difficult to take a single parameter into consideration. There are number of parameters which can directly or indirectly affect the severity or temperature range of T.M.E. They can be broadly considered as

1. > **Variation in composition:** As the alloying elements added to steels can affect as quenched microstructure, the general level of toughness and the transition temperature, this all can affect T.M.E..
2. > **Impurity level:** The impurities are generally segregated at the grain boundaries of material, it becomes necessary to take this as controlling parameter in the embrittlement phenomenon. In such a segregation, the grain boundaries becomes low energy path for crack propagation.
3. > **As quenched Microstructure:** The as quenched microstructure is the source of any transformation taking place during tempering. This may affect the embrittlement mechanism
4. > **Evaluation Methodology for Toughness:** The strain rates involved in two different types of toughness evaluation viz CVN test and Fracture toughness test may change the basic fracture mechanism and may lead to change the T.M.E. temperature and severity.

### 1.4 Objectives of the present investigation:

Considerable amount of work has already been carried out as far as the



effect of composition and impurity levels are concerned. There has been some studies on the effect of testing methodology on T.M.E. There are indications that T.M.E. is negligibly small when evaluated in terms of plane strain fracture toughness ( $K_{IC}$ ) and tempering temperature range of T.M.E. may get shifted to higher values of temperatures when evaluated in terms of  $K_{IC}$ .

In the present investigations AISI 4135 steel has been studied for its Charpy (CVN) and fracture toughness ( $K_{IC}$ ) over the entire range of tempering temperature with the principle aim of finding the effect of two types of tests on T.M.E. and offer an explanation for the observations. The other issues that have been studied are

- (i) The effect of tempering time on T.M.E..
- (ii) Prestrain effect on T.M.E. and
- (iii) Mechanism of T.M.E..

Eventually the study aims to enhance the understanding of the basic cause or causes behind the phenomena.

## Literature Review.

---

In this chapter, literature of the previous papers on TME is reviewed. From this review it becomes clear that the effect of alloying elements and impurity content have been studied earlier in great detail. The microstructure prior to tempering : especially effect of retained austenite, carbide morphology & fractography have also been discussed. The effect of testing methodology i.e strain rate effect and tempering time on T.M.E. is little known.

---

### 2.1) Effect of Alloying Elements:

Systematic research has been made using vacuum melted high purity Fe/C/X steels where X is substitutional alloying element<sup>1</sup>. From this study the substructure of martensite whether dislocated or twinned has been shown to be very important. It has also been shown that this substructure depends on composition, especially carbon and  $M_s - M_f$  temperature range. In general, attempts have been made to use such a composition that will produce dislocated martensite. Thus by proper designing the composition of the alloy, martensite substructure and mechanical properties can be controlled. These were initial steps towards martensitic alloy steel designing. In creating dislocated substructure, small amount of very finely dispersed films of retained austenite was found occupying the interfaces between martensite laths. Furthermore these has been linked to T.M.E. of certain alloy compositions. The detailed information about retained austenite

will be discussed later.

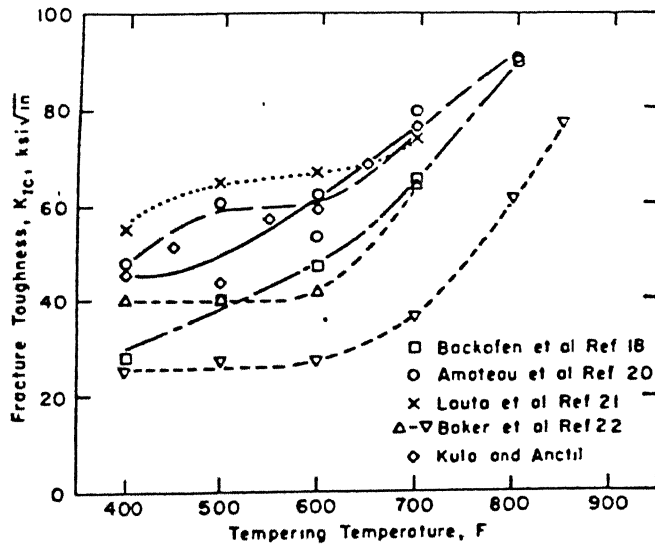
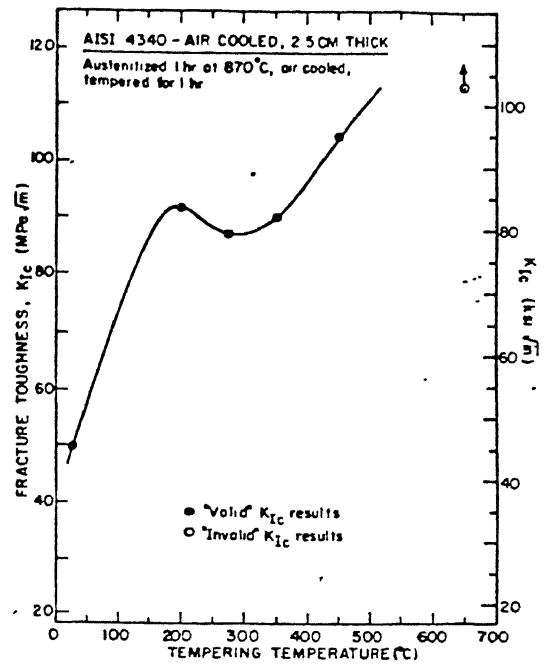
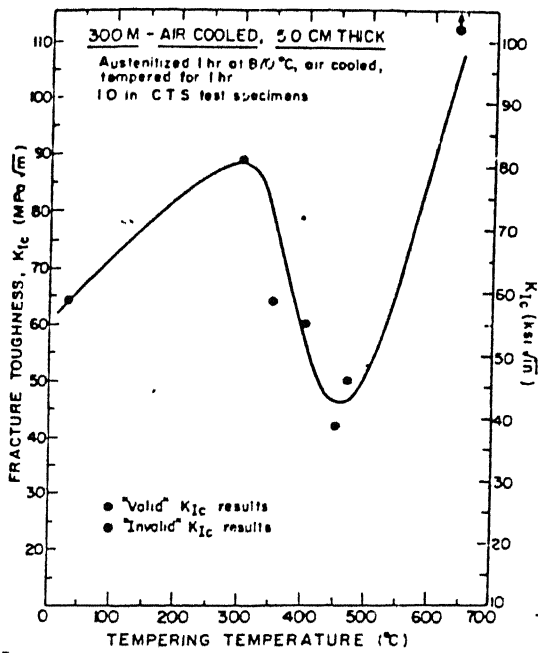
In one study by G. Thomas<sup>2</sup> the plane strain fracture toughness values of Fe/Cr/C system were found to be greater than Fe/Mo/C. In these two different systems retained austenite was detected in former but could not be detectable in latter<sup>3,6</sup>. This difference in retained austenite can be partly due to the fact that Cr is much less potent than Mo in limiting the austenite phase field<sup>6</sup>.

It is also well known that increasing the carbon of steel above 0.5%, increases retained austenite. Mn and Ni are strong austenite stabilizers and are expected to promote retained austenite. The retained austenite was found to be increasing monotonically with Mn addition<sup>7</sup>. Similarly 5% addition of Ni was found to increase retained austenite by about ten times compared to base alloy. These modifications with Ni and Mn tend to improve the Charpy impact toughness values. Thus the composition of steel, in addition to influence martensitic substructure, plays important role in controlling the amount of retained austenite and which was consequently related to T.M.E. and mechanical properties. The T.M.E. phenomena was found to be absent in Fe/Mo/C steels which was also linked to absence of retained austenite in those steels. In another study by G. Thomas<sup>8</sup> it was shown that steels containing high Mn and low Ni content, impact values were wide spread in T.M.E. (i.e wide trough). In case of high Ni steels distinct sharp single minimum was observed. The combined effect of Mn and Si was considered in detail by Bandopadhyaya et al<sup>9</sup>. It has been shown that the degree of T.M.E increases with bulk concentration of Mn and /or Si. The effect of those elements was already considered in temper embrittlement (T.E.)<sup>10,11</sup>. The embrittlement effect of these two elements in presence of "p" is discussed elsewhere.

It was apparent that alloying additions which discourage cementite nucleation and growth can postpone the onset of T.M.E. to higher temperature.

These elements include Ni, Si & Al. The carbon diffusivity in austenite and martensite as effected by the chemical affinity between C and other alloying elements is important. Mn increases carbon diffusivity and promotes rapid nucleation and growth of cementite. Ni, Al & Si do otherwise by discouraging  $M_3C$  nucleation and growth to higher temperature and thus postpone the onset of TME<sup>2</sup>. This was again supported from the experiments by Ritchie et al<sup>14</sup>, in which the shifting of TME temperature range was linked to the effect of Si enhancing the stability of  $\epsilon$  carbide retarding the formation and growth of cementite. This consequently increases thermal and mechanical stability of retained austenite at higher tempering temperatures.

The compositional variations towards T.M.E. was considered in different manner by Knowon<sup>13</sup>. It has been suggested that the factor called *intrinsic toughness* controlled by composition is major parameter in T.M.E. analysis. The various composition studied were of W-Ni steels. Earlier it has been found that W lowers and Ni enhances the intrinsic toughness of steels<sup>9,14,15-18</sup>. It was further found that addition of more Ni can't improve room temperature impact toughness. But the 6W steel having large trough<sup>19</sup> in T.M.E., then modified with Ni additions the toughness loss tend to reduce. Thus addition of Ni produced less brittle fracture in T. M. E. at room temperature & low temperature (-196°C) testing. The presence or absence of T.M.E. was considered to be controlled by this important parameter *intrinsic toughness*. Whenever the alloy composition is such that it has sufficient value of intrinsic toughness the T.M.E. is mostly expected. In this context Ni although improves the intrinsic toughness it causes T.M.E.. This was more apparent in low temperature studies. In contrast to this with low Ni and at low temperature testing T.M.E. was found to be absent but overall toughness was very low.



2—Fracture toughness as a function of tempering temperature for SAE 4340 steel from several different investigations.

Fig. 2.1 T. M. E. Phenomena observed in different alloy composition.

## 2.2 Impurity Content:

In earlier studies of T.M.E. as intergranular fracture mode was predominantly found, role of grain boundary segregation of residual impurity elements was considered to be a major controlling factor<sup>20,21-23</sup>

In earlier 1960's Capus and Mayer were first to reveal the significance of impurities. It was found that alloying additions of Cr and Mn in presence of certain impurity elements such as S, P, and N increased the level of embrittlement. To demonstrate this effect different purity grades of steel samples were tested. T.M.E. was absent for high purity NiCrMo steel but was observed in commercial and doped steels.

Again in 1969, Kula et al demonstrated the existence of T.M.E. in 4340 steel by  $k_{IC}$  measurement. It has been reported that impurity-carbide interaction can be explained in T.M.E.. It was proposed that the impurity atoms at prior austenite grain boundaries are initially incorporated in the cementite and are then rejected from cementite to provide an easy path for crack propagation

A massive work was then done on this impurity effect by Briant and Bannerji which resulted in series of papers from 1978.<sup>23</sup> Concluding about "P" doped steel, it was stated that trough in high purity Ni-Cr steel was absent but it was observed in P segregated samples. The AES studies on prior austenite grain boundaries showed P segregation in commercially and P doped samples. As intergranular P & N concentration didn't increase during tempering it was considered that segregation was inherited from the austenitization treatment. An addition of Mn and Si to high purity steel caused embrittlement and it was attributed to promotion of P segregation in austenite by Mn and perhaps Si. The

T.M.E. minima was always found to be corresponding to maximum in intergranular fracture. In further studies<sup>24</sup>, it was stated that testing temperature if is below transition temperature which is the case of impurity doped steels tested at room temperature, will always show trough.

Considering sulphur effect it was mentioned that even very low bulk concentration of strong embrittling impurities can cause T.M.E. in ultra high purity steels. There was critical austenitization temperature observed, below which embrittlement was absent. This was due to fact that below this temperature sulphur was tied up in the matrix as CrS. Above this temperature the CrS dissolved to grain boundaries. When the cementite precipitation occurred on these grain boundaries which are already weakened by sulphur segregation, the typical T.M.E. at 350° C was observed. The above results were further checked by cooling to lower temperature after austenitization at higher temperature with trough found due to CrS reprecipitation. In another paper<sup>25</sup> it was considered that sulphur segregation depends on austenitization temperature. It was observed that the fracture mode before 350° C tempering was transgranular microvoid coalescence at room temperature testing. At 350° C tempering intergranular fracture with very low fracture energy was found than any other tempering temperatures due to high density of intergranular sulfide. The mechanism of embrittlement found in sulphur doped steels was found similar to P doped steels.

About N segregation it was concluded by same workers<sup>26</sup> that

- 1.) N<sub>2</sub> does not act as grain boundary embrittler (in the Ni-Cr steel studied) in traditional sense. It is almost tied up as nitrides but these nitrides can be quite damaging.
- 2.) If austenitization temperature is low enough (870° C), N is precipitated as CrN<sub>2</sub> at grain boundaries.

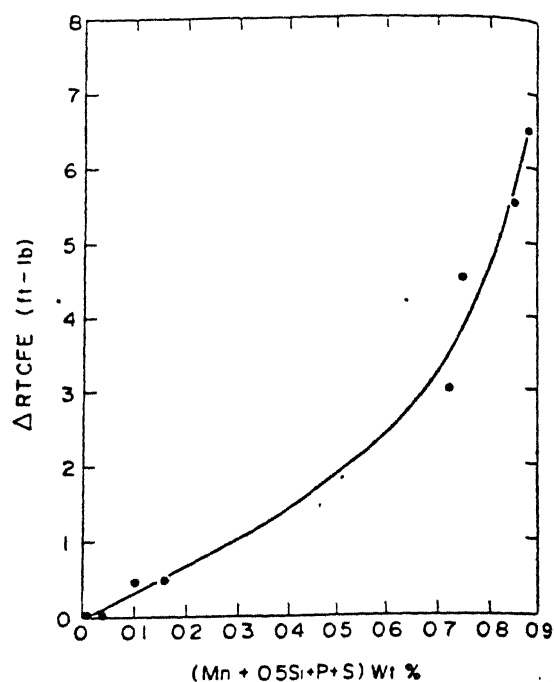
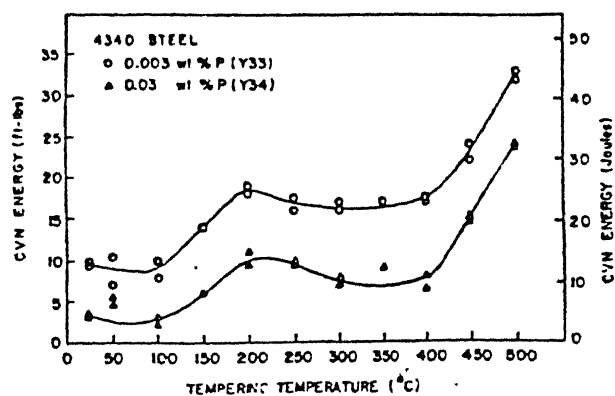
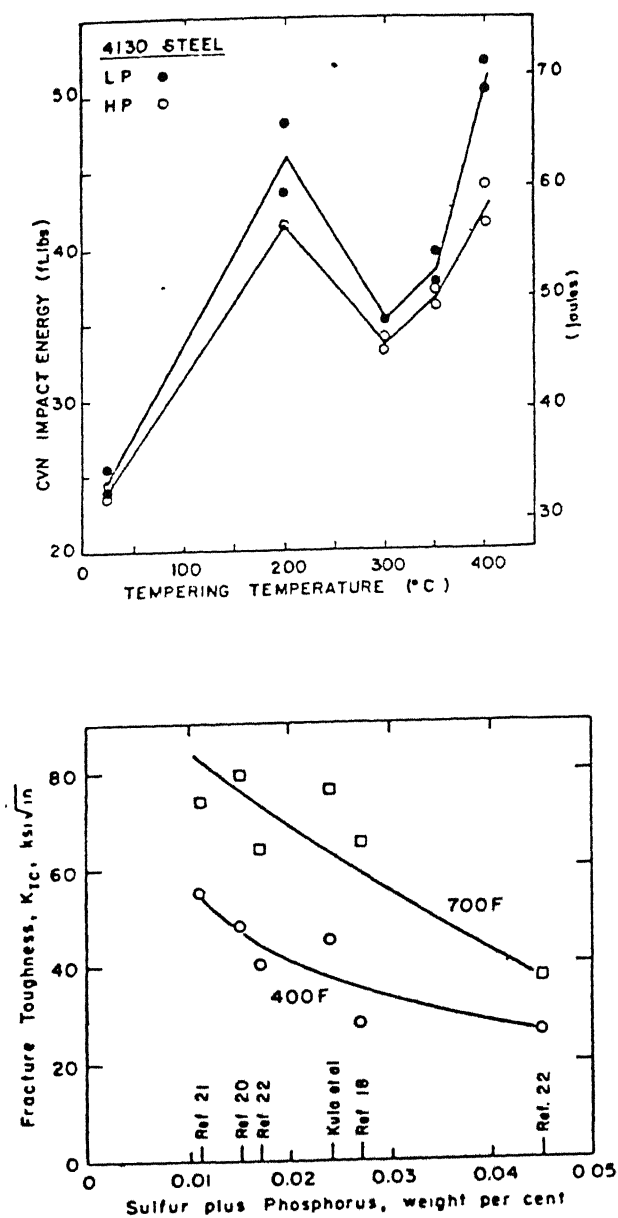


Fig. 13— Variation of the magnitude of Charpy energy trough with composition parameter Mn + 0.5Si + P + S (in wt pct)

Fig. 2.2 Effect of impurity content (S,P) & Mn-Si additions on T. M. E



Below  $250^{\circ}\text{C}$  tempering the fracture energy was found to be low and ductile intergranular fracture was observed. Tempering at  $300^{\circ}\text{C}$  to  $400^{\circ}\text{C}$  results in precipitation of  $\text{Fe}_3\text{C}$  which causes the fracture energy to remain low. Tempering at still higher temperature causes fracture energy to increase due to considerable softening of matrix. Furthermore the coarsening of carbides and nitrides at grain boundaries also aid in ductile intergranular fracture.

In general the steels containing Cr or any other strong nitride forming element, nitrogen will affect mechanical properties because it is precipitated as a nitride rather than it is segregated in its unprecipitated form. Therefore any embrittlement resulting from nitrogen in such a steel will be associated with either transgranular or intergranular ductile failure. An oil quench is sufficiently slow to reprecipitation of grain boundary nitrides.

Even though there has been lot of evidences for T.M.E. as impurity controlled phenomena many papers were also published showing trough even in high purity steels<sup>2,12,27-30</sup> In some paper it was indicated that impurity segregation on grain boundaries alone is not sufficient to cause T.M.E. but the carbide precipitation along with this is necessary.<sup>23,24,31,32</sup>

### 2.3 Effect of Retained Austenite:

The as quenched microstructure of medium carbon low alloy steel, predominantly consists of packet martensite within prior austenite. In earlier studies it has become apparent that small amount of very finely dispersed films of retained austenite occupying about 0.01 to 0.05 volume fraction can be resolved at interfaces between martensite laths in certain quenched and quenched and

tempered experimental and commercial steels by sophisticated electron microscopic methods<sup>3,7</sup> The observation of such austenite had been linked to fracture toughness properties and empirically it had been shown that thermally stable retained austenite can be beneficial.<sup>3,4,7</sup> T.M.E. trough found in certain alloy composition was also linked with retained austenite decomposition forming interlath carbide films

The effect of alloy composition on retained austenite is already mentioned in earlier sections. Heat treatment also plays a key role in determining retained-austenite. Higher austenitisation temperature is found to increase the retained-austenite<sup>3,7</sup> It was found that substantial amount of retained austenite can be introduced in microstructure by holding the steel in martensite formation region ( $M_S$ - $M_f$ ) during quenching.<sup>36</sup> Although the grain refinement could decrease the severity of T.M.E., the thermal stability of retained -austenite was unaffected and occurrence of toughness minima can be expected even in fine grained alloys It has been further indicated by G.Thomas<sup>2</sup> that whatever benefits of retained austenite , are lost if it is thermally unstable. The austenite stability with respect to transformation to martensite on quenching must be related to -

- 1). Between  $M_S$  -  $M_f$  ; the solute elements ; especially carbon will segregate to austenite thus lowering  $M_S$  and also  $M_f$  locally further and further down leading to untransformed austenite (chemical stabilisation).
- 2) Accomodation of transformation strains by plastic deformation generating dislocations in austenite could also stabilise the austenite through mechanical stabilisation<sup>34,35</sup>

The stability of the austenite with respect to decomposition into  $\alpha$ - $M_3C$  will decrease as the carbon content in austenite increases due to a higher chemical driving force for carbide nucleation. Thus those factors which minimise austenite

to martensite transition will favour austenite to carbide transition

The retained -austenite decomposition effect related to T.M.E. was then discounted due to the fact that

1) Sub-zero treatment (which removes most of the retained -austenite) did not eliminate T.M.E.<sup>36</sup>

2.) There was no retained -austenite transformations involved in intergranular failure mode observed in T.M.E.

Role of retained -austenite on T.M.E. was then focussed in different way, based on the new data concerning distribution, morphology and thermal and mechanical stability of retained -austenite during tempering.<sup>2</sup>

Ritchie et al<sup>12</sup> have concluded stability of retained -austenite with respect to tempering temperature, the presence of retained -austenite can play major role in the onset and severity of the T.M.E.. Furthermore, it had been shown that irrespective of initial heat treatment procedures, the T.M.E. coincided with range of tempering temperature where retained -austenite becomes mechanically unstable with respect to deformation. The earlier consideration of G. Thomas of just thermal stability was not accepted fully, as it was found that retained -austenite was still present in unstressed specimens even upto 450 ° C (300 M steel). Although some fraction of retained -austenite transforms during tempering, large amount remains thermally stable but mechanically unstable due to carbon depletion and then transforms on subsequent loading.

About beneficial role of retained -austenite<sup>2,7,37</sup>, Ritchie et al, have discounted it, with the facts that before claiming any beneficial role, it is essential to define the stability of the austenite both thermally and mechanically. In both cases either it transforms to interlath cementite or untempered martensite

which result in massive trough.

Work by Badheshaha and Edmonds<sup>3</sup> showed that retained austenite was present in Fe-Mo-C alloys and was stable upto - 196° C refrigeration for 1 hr. This disagrees with Clark and Thomas<sup>2,5</sup> who did not find any retained austenite for similar composition & also T M E was found to be absent. Study on Fe-1.8V-0.25C alloys by Badheshaha et al<sup>5</sup> showed inter-lath films of retained-austenite & embrittlement trough was well defined as compared to Fe-Mo-C steels. Tempering of above alloy at 290° C revealed that retained-austenite decomposes into laths of cementite at martensite boundaries. At 350° C (within T M E trough) limited coarsening of inter-lath cementite was detectable. Also as at 290° C all the retained-austenite had decomposed, impact curves had not showed full embrittlement & embrittlement was rather more complete at 350° C. Another distinct conclusion of the same workers showed that mechanical instability of retained-austenite has no role in either Fe-Mo-C or Fe-V-C type steels, since not only embrittlement was present in absence of retained-austenite (due to tempering) but the embrittled toughness values fell below those of the as quenched specimens.

Again the model suggested by Sarikaya et al<sup>6</sup> indicated that the stability of the retained-austenite is of primary significance in controlling the properties. The carbon partitioning was found in retained-austenite where Carbon levels of austenite raised above 2.5% and more than 5% at martensite/austenite interface. Bainite-like structure was another interesting feature of observations, but the mechanism of the formation of this phase was not clarified. The instability of the retained austenite was analysed by T.T.T. diagrams. Two such T.T.T. curves for 0.3% and 1% of carbon were plotted simultaneously. The tempering of 0.3% carbon steel to 300 to 400° C, in

which retained-austenite had decomposed corresponding to well above the  $M_s$  temperature on carbon enriched retained-austenite (approx  $120^{\circ}\text{C}$ ) and was found to be in bainitic region. The resulting microstructure was discontinuous stringing of carbides at lath boundaries due to austenite decomposition and so similar to upper bainite structure<sup>56</sup>. Thus, austenite can change the kinetics of transformation.

According to work done by Bandyopadhyay<sup>55</sup> on the role of retained austenite in the T M E range, the transformation of austenite leads to decrease in maximum stress in front of notch. It was further noted that for a particular steel there was smaller drop in value of max-stress for larger austenite transformation.

Another steel showed smallest amount of retained austenite but largest value of max-stress. Thus, it shows that the retained austenite was not the factor to increase the toughness. This correlation of retained austenite transformation (by magnetic measurements) and max-stress value was found to be quite different for low temperature test. The retained austenite at prior austenite grain boundaries is one of the cause stated by Sastry and Wood<sup>58</sup> for T M E, when the austenitisation temperature was  $1200^{\circ}\text{C}$ . As usual practise, the austenitisation temperature is  $850^{\circ}\text{C}$ , in which very little austenite would be found at grain boundaries the above reasoning was denied by Bandyopadhyay et al<sup>59</sup>. The region of 0.4% carbon, retained austenite decomposition produce less than the 10% vol.fraction of carbide. Furthermore the thickness of retained austenite found was not greater than 0.05 microns. It therefore implies that the resulting carbide must be of  $50\text{ \AA}$ . Such a films are assumed to exacerbate the effect of sulfure or Phosphorous. The thickness of carbide films found by Bandyopadhyay et al<sup>59</sup> were of different size & so assumed to be due to decomposition of martensite & not by austenite.

## 2.4 ROLE OF CARBIDES & NITRIDES:

First it was Grossman<sup>40</sup>, who proposed definite link between sequence of carbide precipitation and TME. Again Kinglev et al<sup>41</sup> suggested embrittlement was concurrent with formation of platelike carbides replacing epsilon Carbide. Many workers related TME with coarsening of carbide films ( $\text{Fe}_3\text{C}$ ) which were generally observed to form at grain and lath boundaries<sup>42</sup>. Further more interaction of dislocation density and coarse carbide has been found TME trough was displaced to higher tempering temperature in steels fractured below room temperature.

Rigorous study of T M E showed an important feature that, for all treatments epsilon- carbide, identified as the hardening carbide at peak strength (& peak toughness) was replaced by cementite in embrittlement range. Furthermore it was shown that cementite had precipitated as discontinuous films. From the study of B & E inter-lath cementite precipitation in Fe-Mo-C alloys tempered at  $190^\circ\text{C}$  was found. The lath boundaries did not reveal any cementite precipitation (although retained austenite was found). So T M E was considered due to inter-lath cementite in such type of alloys. At higher temperatures above  $295^\circ\text{C}$  retained austenite decomposed to give cementite films. These films were found to be discontinuous as they came from  $100\text{ \AA}$  thick retained austenite films. The cementite nucleates at several positions of austenite /martensite interface, so the final decomposition product was small discrete cementite particles at inter-lath boundaries. The cementite was found to be oriented with respect to martensite matrix which is energetically favoured also it was in contact with both martensite & austenite. The microstructural observations around both the cracks indicated crack nucleation role of

cementite rather than easy fracture path. Ni-plated fracture surface of above composition showed trans-lath fracture indicating similar crack nucleation role of cementite. Analysing carbide effect on TME<sup>25</sup> expressed that even though the intergranular fracture was found in high P (also by Banerji et al<sup>23</sup>), it could be possible only after tempering above 200° C. Thus presence of P at grain boundaries by itself, is therefore not sufficient to cause TME. A tempering reaction at austenite grain boundary is of austenite decomposition to cementite and ferrite or cementite precipitation from tempered martensite is also necessary to produce TME associated with impurities and intergranular fracture. There was no evidences of cementite at prior austenite grain boundaries and therefore it led to conclude that the fracture must be transgranular for low P steels.

From the observations by Briant<sup>43</sup> the extraction replicas of specimens in TME range showed increase in carbide density (especially at 300° C), with higher tempering temperature the density was found to be still higher. In all cases the carbides were ribbon shaped and of  $M_3C$  type. The X-ray spectrum on analytical electron microscope showed that the carbides were  $Fe_3C$  and no alloying elements were introduced. Critical observations about carbide thickening showed that it occurs with increase in temperature and also decrease in number of carbides below 0.01 micron was observed. The carbides near the grain boundaries were no thicker than those found in matrix, but they were significantly long. The length found for matrix carbides was typically in the range of 0.3 to 0.6 micron and those found at the grain boundaries were 1 micron long. Both inter and intragranular carbides appear equally predominant after tempering at 250° C and 300° C. It is only after higher temperatures, the length of the grain boundary carbides become significantly greater than

those in matrix. As the temperature of tempering is increased the carbides along the grain and lath boundaries become more closely spaced. Although  $450^{\circ}\text{C}$  tempering should produce spheroidization, Briant had found similar ribbon shaped carbide morphology. Also no incorporation of alloying elements in carbides was found even at  $450^{\circ}\text{C}$  tempering. The extraction replicas of as quenched specimens also showed  $\text{Fe}_3\text{C}$  or  $\text{Fe}_2\text{MoC}$ , which were the undissolved carbides formed & retained after normalising & austenitising. The Mo & Cr partitioning into cementite during pearlite formation had already been found. For such experiments cooling rates were slow enough to permit partitioning of alloying elements into cementite & also these carbides are more stable than cementite. In most of the cases large microvoids were formed at inclusion particles & were joined by smaller voids nucleated at fine undissolved carbides. The concentrated shear band between the crack tip & large voids opened up many very fine microvoids at the undissolved spherical carbides. In absence of these fine particles, large void may either grow to join the crack tip or fracture may occur by shear decohesion between the void & crack tip. Thus fine undissolved carbides also play an important role in ductile fracture. Further Curry & Pratt<sup>44</sup> had shown that the nucleation rather than growth of fine voids at carbides is critical process during ductile crack extension.

It was shown by Briant<sup>43</sup> that carbides can aid in all three types of fracture i.e. ductile, intergranular and cleavage and in all cases it decreases the fracture energy.

- 1.) The cleavage type fracture can be produced by carbides.<sup>45</sup> The cracks produced in carbides if grows long enough to propagate into matrix leads to cleavage. Thus the carbides must be larger than critical size, if they are to initiate cleavage otherwise



the cracks formed in the carbides will be too small to propagate into matrix

- 2) The carbides also can aid ductile fracture to decrease the toughness (as was found by Cox et al.<sup>46</sup>) In such a situation small microvoids formed around the carbides help in linking up the larger microvoids formed around inclusions. If the carbides are not present, these microvoids around the inclusions will grow until they coalesce; but introduction of small microvoids around the carbides allows microvoids to be connected at lower strains.
- 3) It is also assumed that the carbides aid in intergranular fracture, but has no evidences. The carbides either could provide locations against which the dislocations could pile-up to initiate a crack along an impurity-weakened-grain boundary or they could crack, as for cleavage fracture. When grain boundaries are weakened by impurities, the crack would proceed along them rather than matrix. There must be critical size of carbides to initiate such a intergranular fracture. The carbide/matrix interface at grain boundaries are more easier path to propagate than without precipitation of carbides.

In study of commercially pure 4340 steel, Briant<sup>43</sup> found that the fracture mode was ductile below 300°C tempering. The fracture surfaces showed very fine voids that had sizes typical of precipitated carbides. Thus carbides aid in ductile to decrease the toughness between 200°C to 300°C (initial T M E). A similar mechanism was proposed by Schwalbe and Backfisch<sup>47</sup> who were able to relate a decrease in fracture energy with decrease in void size measured from carbon extraction replicas.

For low P steels no intergranular fracture was observed in as quenched steels but maximum amount of intergranular fracture was observed only after tempering temperature of 350°C. Thus it was suggested by Briant<sup>43</sup> that for a given level of segregation (depending on initial impurity content and tempering temperature) of an embrittling impurity, there will be a critical carbide coverage in terms of size and population required to produce intergranular fracture. As only specimens of high and low toughness values in T M E range were examined, it is difficult to correlate gradual increase in intergranular fracture between these two tempering temperatures.

## 2.5 Fracture Modes:

There has been lot of work performed to analyze the fracture modes occurring around T. M. E. Some of the findings are tabulated in the next page & critical points are reported here.

The sudden decrease in ambient temperature Charpy V-notch impact energy & an increase in Charpy transition temperature during tempering was historically associated with an increase in intergranular fracture during failure.<sup>40,41</sup> However, later work showed that fractures in TME range were not always intergranular; other modes such as cleavage, quasicleavage, fibrous, mixed ductile-brittle, martensite translat, interlat/packet were observed.

It was clearly demonstrated by Horn et al<sup>12</sup> that intergranular fracture is not necessarily a characteristic of T M E, particularly in commercially important steel. The various mechanisms leading to various fracture modes are considered

by Ritchie & Horn<sup>12</sup>; they are

#### Trans-granular Cleavage:-

when the level of impurities & retained-austenite is small, the dominant embrittlement mechanism is the tensile fracture of carbides, resulting in trans-granular cleavage.

#### Interlath- Cleavage :-

Consequence of interlath carbide precipitation is mechanical destabilisation of remaining inter-lath austenite, resulting in largely stressed assisted transformation to an inter lath layer of untempered martensite. This provides major contribution to embrittlement resulting in inter-lath cleavage fracture mode

#### Intergranular fracture :-

From studies of Banerji<sup>23</sup>, in steels containing sufficient residual impurity content, or microstructure particularly susceptible to grain boundary embrittlement ( i.e. coarse grained structure ) ; such impurities particularly P, will tend to segregate to prior austenite grain-boundary during austenitisation. In the embrittlement range , the combination of cementite precipitates & impurities at prior austenite grain boundaries will lead lowest cohesion at carbide/matrix interfaces ( near grain boundary ) resulting inter-granular cleavage.

### Mixed mode or fibrous fracture mode :-

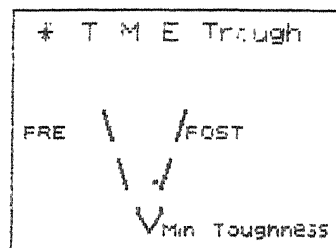
If the temperature of testing is above the ductile / brittle transition temperature then mixed or fibrous fracture mode may result.

It was seen by Materkowski et al.<sup>25</sup> that the size of cleavage facets was of the order of the martensite packet size and was considerably larger than the size of fine quasicleavage facets observed in as quenched specimens. Furthermore by finding large amounts of cleavage, which was transgranular to prior austenite grain structure. The interlath fracture mode which was found by earlier workers<sup>2,12</sup> was disagreed.

Although in TME, the retained austenite decomposition was being assumed, the fracture mode was found to be across the carbides rather than along the carbide matrix interfaces or along the lath boundaries. Such a fracture mode found to be associated with plate shaped carbides, is observed in extraction technique from the fracture surfaces in 4340 steel. Similarly, translath cleavage had been observed in TME of 0.6% C steel by King et al.<sup>27</sup> The findings of Smith et al.<sup>27</sup> showed that, the interlath carbides apparently crack first under load and initiate cleavage cracks on most favourably oriented cleavage planes at the martensite packets.

The fracture mode observations by Briant<sup>43</sup> for samples tempered at 250°C showed trans-granular features with large elongated voids centered on MnS inclusions and finer voids between them. The tempering at, and above, 350°C produce significant intergranular fracture mode. Although in TME range the impact value is decreasing constantly, intergranular fracture was found only at 350°C. Fracture surface morphology was observed to be changing in specimens at 200°C, 250°C, 300°C. The small voids, for higher magnification, were located between the larger voids around Mn-S inclusions which were circular.

and uniform in size. The small voids (0.1 to 0.5 micron dia.) were exactly matching the size of carbides which were precipitated in T M E range. Thus, it was shown that tempering in T M E range produces more sites for void nucleation, which causes ductile fracture energy to decrease.



## Fracture mode analysis with Tempering Temperature for different Steels

Material	As quenched	* Pre	* Minimum toughness	* Post	Ref No
300-M oil quenched	Ductile microvoid coalescence Intergranular Transgranular Cleavage.	Ductile rupture 300°C	Ductile rupture 400°C	Ductile rupture	12
300-M Air Cooled	-----	" "	Lath Boundary Cleavage	-----	" "
4340 Oil quen.	-----	Ductile rupture 200°C	Fully Trans-granular Cleavage 275°C	-----	" "
Fe/V/C	-----	Ductile rupture	Quasi cleavage	-----	2
Fe/V/C	Ductile rupture	<u>Quasi cleavage</u>		Ductile rupture	9
4340 High P Low P	Quasi cleavage 20 % Intergranular -----	microvoid coalescence 200°C -----	Mostly Intergranular 350°C Cleavage	-----	28
Fe/Cr/Mn	-----	Ductile rupture 210°C	Quasi cleavage 350°C	Quasi cleavage 400°C	8
com 4340	-----	Trans-granular	Intergranular	-----	43

## 2.6 Effect of Evaluation Methodology:

There has been very little work done about evaluation methodology especially to see its effect on the T.M.E.

Walker and May<sup>45</sup> have not found a minimum in room temperature  $k_{IC}$  values in N-Cr-Mo-V steel. Materkowski et al<sup>46</sup> working on high and low "P" 4340 steel, have found no T.M.E. trough in  $k_{IC}$  testing for low "P" content steel. A narrow transition zone had been found between pre-crack and overload fracture surface of compact tension specimen. The zone was very narrow and was consisting primarily of ductile fracture. This was followed by brittle cleavage mode. The improvement in toughness values was attributed to this narrow zone to the lowered rate of work hardening and the associated ease of dislocation motion. The yield and fracture stress of martensitic steel tend to approach each other with increasing tempering temperature. It is an indication of reduced work hardening that develops on tempering and had been related to dislocation interaction with the coarse carbide particles that develop in martensite on tempering. Swarr and Krauss<sup>50</sup> found that as quenched specimens was due to the development of well defined dislocation cell structure, while the low rate of work hardening of tempered specimen was related to maintenance of relatively low uniform array of dislocations. The ready bypassing of carbides in tempered martensite prevented the accumulation of dislocations into a cell structure with increasing deformation.

Materkowski et al<sup>46</sup> showed that the low rate of work hardening in low "P" 350° C tempered specimens permit the development of large amount of strain around carbide particles during the initial loading and crack extension of  $k_{IC}$  test. It therefore produces the observed zone of microvoid coalescence.

About inconsistency in T.M.E. evaluation ( $k_{IC}$  and CVN testing), Zia et al<sup>49</sup>

indicated that the  $k_{IC}$  testing attempts to measure a material property related only to the extension of an unstable crack. In C/VN testing various aspects of fracture are evaluated, including both ductile and brittle crack extension. The complex fracture induces an additional difficulty in comparison of two different methods.

In very recent study a new technique of *dynamic toughness testing* is being introduced<sup>51</sup>. In general it was observed that the steel is tougher under dynamic loading than in static loading for all tempers. This was found to be more prominent at high temperature studies. Dynamic loading results in a shift of the ductile to brittle transition temperature towards higher temperature. There is little influence of strain rate on the flow stress level in shear but it has strong influence on ductility of material. There is considerable loss in ductility with higher strain rates. It must be noted that only peaks of fracture initiation energy are recorded in dynamic testing and no energy is being accounted for crack propagation. This is fundamentally different from usual Charpy toughness test. Another interesting feature of this dynamic loading was that no T.M.E. trough was found even after clear indication of carbide precipitates. The T.M.E. can only be found when test temperature is below transition temperature. The static testing produces less pronounced trough. For 350° C temper, tested at room temperature and above showed fibrous fracture mode in both dynamic and static loading but higher fracture stress in dynamic than static was attributed to higher flow stress that prevail at higher strain rate. Chi et al<sup>52</sup> found no trough at 350° C in  $k_{IC}$  testing, But the T.M.E. was observed with more pronounced trough in dynamic testing at low temperature.

In another recent study by Lee et al<sup>53</sup>, it was stated that shallow trough (less severe) can be found in  $k_{IC}$  testing as compared to CVN testing. Crack tip



blunting of  $k_{IC}$  specimen was observed and was related to void formation around MnS inclusions. As these voids grow, the deformation becomes localised into intense shear bands between the voids. If a fine dispersion of carbides is also present in the matrix, then the high strains within shear bands also can cause microvoids to form at carbide matrix interfaces. Voids will form within shear band and fracture will occur. As the larger inclusions were placed wider, more pronounced role is played by carbide particles closely spaced, in determining  $k_{IC}$ . Thus the decrease in  $k_{IC}$  brought about by tempering at 350° C is attributed mainly to decrease in spacing of carbide (cementite). At higher tempering temperature the carbides are more spheroidal and larger, so are not able to nucleate as many voids. Also the steel becomes softer leading to improve the  $k_{IC}$  values. This was further verified by high austenitisation temperature studies.

Comparing the two different toughness values ( $k_{IC}$  and CVN) it was observed that larger amount of intergranular fracture was present in CVN tested samples than  $k_{IC}$ . This needed careful observation in two different situations. It is also well known that each has its own associated stress field in fracture origination regions, strain rate, and specimen dimension requirements. In Charpy test as stress controlled fracture process i.e. quasi-cleavage and intergranular fracture was present ahead of blunt notch, the T.M.E. was attributed to decrease in fracture stress. Fractographic evidences has also indicated that for Charpy samples in T.M.E. range (350° C), fracture initiation and first stage of crack propagation occur mostly by stress assisted fracture to intergranular type and this lead to conclude that the crack initiation is created by carbides and then propagated by intergranular cracking through the weak grain boundaries due to "P" effect.

## 2.7 The Testing Temperature and T.M.E.:

Although the T.M.E. has been found at room temperature testing it became necessary to see the effect of testing temperature on the most critical phenomena.

Ripling<sup>54</sup> showed the importance of test temperature as a criterion for evaluating T.M.E. on unnotched tension specimen, he found no discontinuity in room temperature testing for all tempers. At low temperature testing minimum in properties like reduction in area and fracture stress for 500 F temper was observed. Rickett & Hodge<sup>55</sup> were the first to show by impact testing carried out over a range of temperature that T. M. E. was manifestation of the change in transition temperature with tempering temperature

Laut & Stoughton<sup>20</sup> studied the tensile & fracture toughness of SAE 4340 steel as function of tempering temperature & test temperature. They attempted to relate  $K_{IC}$  to the strain hardening exponent.

From the study of Kula et.al<sup>20</sup>, it was observed that severity of T. M. E. depends on several factors relating to surface resulting from the three dimensional plot of toughness (energy) ,test temperature & tempering temperature. These are :

- \* The reference or test temperature & it's relation to transition temperature ,
- \* Rate of change of transition temperature with tempering temperature ,
- \* Rate of change of energy value with tempering temperature , both above

& below the transition .

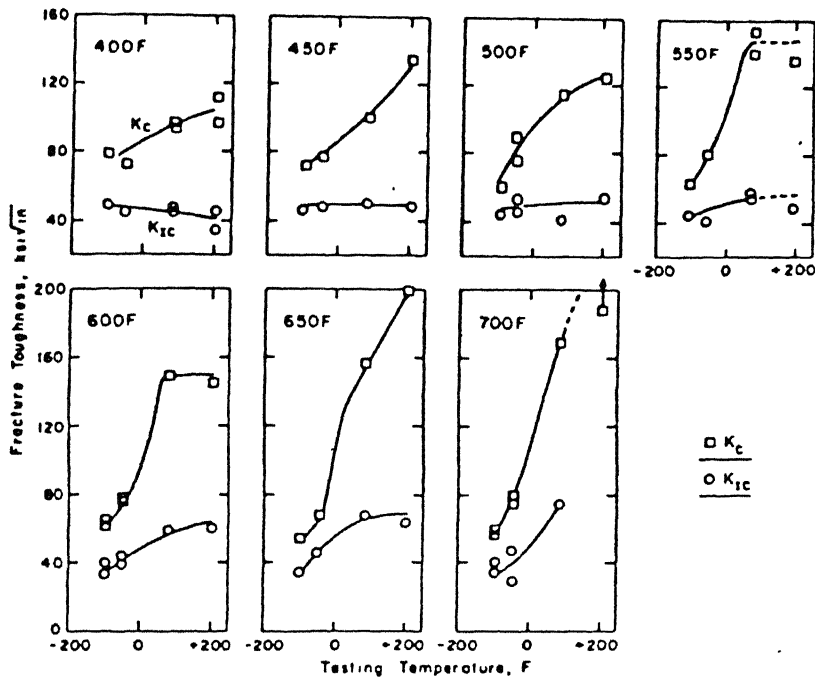
\* The sharpness of transition temperature region.

A narrow transition region , a large change of transition temperature with tempering temperature & test temperature lying within the transition temperature will all tend to give a greater manifestation of embrittlement .

For Charpy test , the transition region may not be sharp in case of high strength materials. Unfortunately there is little information on transition temperature for fracture toughness values. Although it has been found that the  $K_{IC}$  values does vary with test temperature , the transition is less sharp , if a transition in it's true meaning does exist at all.

From the study of high & low P content of steel it was shown that transition temperature is raised by P strongly.<sup>28</sup>

It was suggested by Bandyopadhyay et al<sup>39</sup> that the shift in transition temperature due to 350° C vs. 250° C tempering shows that the room temperature is in transition range for 350° C ; but not for 250°C tempering .So energy minimum should be observed at all test temperature below room temperature for 350° C tempering. It was again confirmed that transition temperature goes through a minimum corresponding to minimum in fracture energy.<sup>55</sup> The actual minimum in  $K_{IC}$  values from two different studies by Kula et. al<sup>20</sup> & King et al<sup>27</sup> was found for higher tempering temperature specimens tested at low temperatures.



—Plane stress and plane strain fracture toughness as a function of testing temperature for various tempering temperatures.

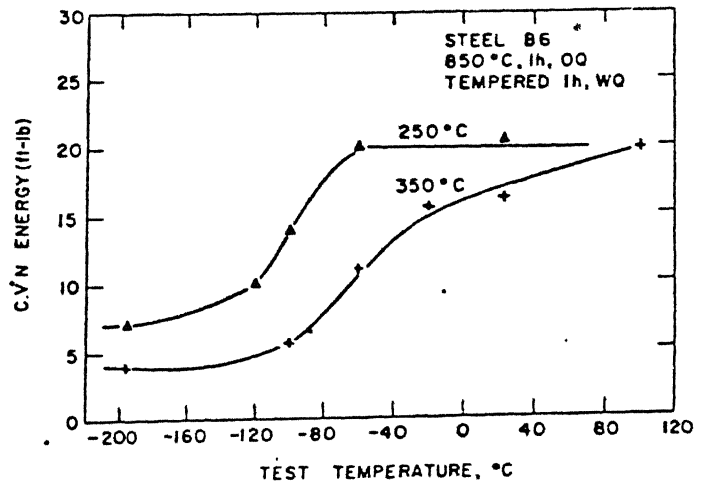
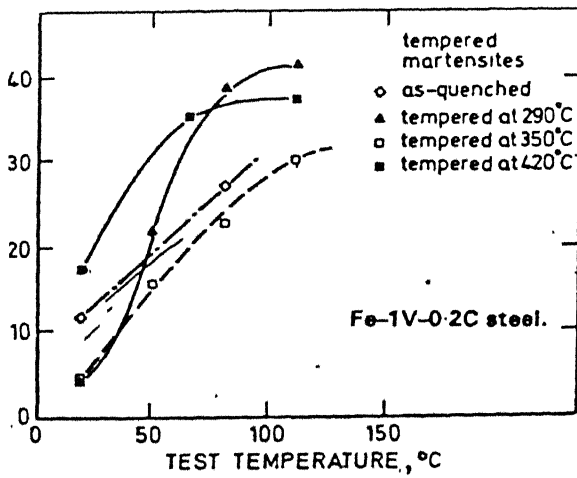


Fig. 2.3 Effect of Testing Temperature on T. M. E.

## 2.8 Effect of Tempering Time:

The tempering operation is temperature and time dependent. Tempering at different time may change the morphology and fracture behavior of tempered martensite. But there has been very little research towards this issue.

This factor has been considered by G Thomas<sup>8</sup>. It has been shown that tempering for very long time (1315 hrs) at 400° C, for Mn containing steels, change the fracture mode from quasi cleavage with many "ridges" to intergranular fracture which is the case of T.E. The impact values dropped with increasing time at temperature within T.M.E.. The intergranular fracture was not observed for 1 hr tempering in all temperatures within T.M.E. Again this was supported by Horn<sup>12</sup> stating that T.M.E. is time dependent at different temperatures i.e. we may get embrittlement if longer time is provided below T.M.E. temperature range. Importance of time has been overlooked in different way Nakashima et al<sup>42</sup>. The studies show rapid induction heating and cooling will suppress the embrittlement. It was assumed that the globulisation of cementite particles during third stage, will reduce the effect of embrittlement otherwise due to elongated ribbon shape. The globular structure is expected to increase toughness values. During induction tempering the high heating rates (i.e. very small time) associated with stress gradients influence the nucleation and growth of the cementite. A greater nucleation sites may contribute to a wider distribution of the cementite while very short time may minimize the growth of elongated films.

## 2.9 Mechanisms of T.M.E.:

As the work on T.M.E. has proceeded various mechanisms have been proposed. Some of the mechanisms points towards factors considering particular cases. As there are various factors involved in T.M.E. a generalized solution have not yet been successful found out. Some of the mechanisms put forward are discussed here

### 1.) Ferrite Grain Boundry Network :

Grossmann<sup>57</sup> noted that the fracture surface of embrittled steels contained many bright, intercrystalline facets. From metallographic observations, he concluded that a ferrite grain boundary network was responsible for the embrittlement, and not retained austenite, which had been an earlier view.

### 2.) Precipitation Of Cementite :

Kingler et al<sup>41</sup> observed that embrittlement was a time-and-temperature-dependent phenomenon and was associated with the early stages of precipitation of cementite from martensite. They felt that localized precipitation of cementite at prior austenite grain boundaries and the ferrite network surrounding this cementite was the cause of the embrittlement.

### 3.) Inter-lath Carbide Film :

It was suggested by Lement et al<sup>58</sup> that a continuous carbide film at martensite plate boundaries forming in this temperature range could be the cause of embrittlement.

Nakashima and Libsch<sup>42</sup> found that tempering by induction heating avoided

tempered martensite embrittlement and also tended to form globular carbides at the start of the third stage of tempering.

The association of embrittlement with the precipitation of cementite was also confirmed by the effect of silicon on tempering. Altan and Payson<sup>55</sup>, Shih et al<sup>60</sup> and Alstetter et al<sup>61</sup> showed that an increase in silicon content raised the temperature at which cementite formation began and also raised the temperature for the minimum in impact energy.

Thermomechanical treatments, such as the formation of martensite in cold-worked austenite, have been found to alleviate the tendency toward embrittlement on tempering by shifting the impact transition curve to lower temperatures<sup>62</sup>.

#### 4.) Impurity Element Effect :

Considerable evidence has been gathered, especially by Capus<sup>21,63</sup>, that impurity elements play an important role in controlling embrittlement. High-purity steel shows no tempered martensite embrittlement, and the transition temperature decreases continuously with increasing tempering temperature. Additions of certain impurity elements, phosphorus, arsenic, antimony, tin, nitrogen, and silicon may lower the supertransition energy level and give rise to a maximum in the transition temperature at some intermediate tempering temperature.

Then after, transmission electron microscopy was used to study the structure of steel tempered in this range. Baker et al<sup>64</sup> noted that the improvement in toughness on tempering beyond the 500 F embrittlement range was associated with a spheroidization of carbide particles at martensite and twin boundaries, recovery in the high dislocation density array, and elimination of the twin boundaries. The actual embrittlement was aided by preferential paths for crack propagation provided by the carbide films.

#### 5.) Precipitation & Dislocation Interaction :

Somewhat different conclusions were reached by Banerjee<sup>65,66</sup>. He concluded that tempered martensite embrittlement (as well as temper brittleness, which occurs in certain steels at about 1000 F) was associated with the simultaneous resolution of a metastable precipitate and reprecipitation of a more stable precipitate. He felt that a higher dislocation density, together with locking of the dislocation intersections and jogs by the precipitate, was the cause of the embrittlement.

#### 6.) Change In Fracture Mode :

Bucher et al<sup>67</sup> have studied the structure of high-strength steels by electron fractography. They showed that the fracture surfaces of Charpy impact specimens tempered in the embrittlement range contained high proportions of grain boundary fracture (upto 40 %), whereas the fracture surfaces of specimens tempered below and above this range were predominantly dimpled rupture of cleavage. These results strikingly confirmed the relationship between tempered martensite embrittlement and grain boundary fracture.

#### 7.) Mech Instability of Retained Austenite:

According to conclusions stated by Horn et al<sup>12</sup>, T M E was considered to be combined effect of mechanical instability of inter-lath films of austenite & replacement of epsilon-carbide by precipitation of inter-lath cementite. Carbide was seen at the same locations as films of high carbon austenite. This high carbon retained-austenite on lath boundaries can then act as primary source for the precipitation & growth of embrittling carbide films at austenite - martensite lath interfaces. Once the carbide forms, the austenite



becomes depleted in carbon & accordingly becomes mechanically unstable; it was shown by change of retained-austenite lattice parameter with carbon depletion. On deformation the unstable austenite transforms to leave an embrittling films of untempered-martensite on lath boundaries in same locations as embrittling cementite precipitates. When retained-austenite is less, embrittling effect of inter-lath cementite was shown by trans-granular cleavage fracture mode, presumably initiated by the tensile cracking of grain boundary / inter-lath carbides. For large amount of retained-austenite fracture mode was inter-lath cleavage showing dominant role of retained-austenite than carbides.

#### B.) Coarsening of Carbides:

From the study of Bhadhesia et. al<sup>9</sup>, it was shown that in earlier stages of embrittlement when retained austenite had not decomposed, T.M.E. was controlled by intra-lath cementite. Even at 295<sup>0</sup> C. The decomposed cementite is not coarse as inter-lath cementite. At 480<sup>0</sup> C, coarsening of inter-lath cementite was observed, which was considered for controlling T.M.E.. Furthermore different controlling factors operates in different compositions. In case of Fe-Mo-C steel, the coarser intralath cementite acts as controlling factor in T.M.E. and retained austenite or its subsequent decomposition product, i.e., finer dispersion of interlath cementite has no effect as such. For Fe-V-C steel as it contains more retained austenite and the T.M.E. is assumed to be attributed to coarsening of inter lath cementite formed due to decomposition of retained austenite. In Fe-Mn-Si-C system as retained austenite is completely absent it gave only intralath carbide (very fine due to Si) and no embrittlement due to transition from epsilon to cementite. This also suggests beneficial role of Si for temper resistance.

### 9.) Thermal Instability of Retained Austenite:

From the study of G. Thomas<sup>6</sup>, T.M.E. was assumed to be associated with the decomposition of retained austenite into carbides at the lath boundaries due to its thermal instability. This instability was assumed due to thermodynamical requirements associated with the carbon levels retained after quenching. The main factor affecting fracture in T.M.E. was appeared to be the size and microstructure on slip distribution and crack initiation. The carbides so formed restricted the slip with the lath and did not permit easy crossing of slip from lath to lath unlike the strongly influenced by the austenite decomposition.

### 10.) Intergranular Carbide Failure:

The contribution made by inter-lath carbide for embrittlement, initially suggested earlier<sup>12,27,28</sup>, wasn't assumed to be of major significance by Bandyopadhyay et al<sup>39</sup>. As T.M.E. was found to be correlated with intergranular fracture (due to precipitation mechanism for T.M.E. was considered to be the transformation of intergranular retained-austenite was not considered as a controlling factor. The toughness minima was found to be consequence of reduction of retained and T.M.E. was not given, the presence of carbides at prior austenite grain boundaries, which were already weakened by segregated impurities lead to T.M.E.

The mechanisms of T.M.E. concluded by Zia et al<sup>69</sup> suggested that it is not only associated with brittle type fracture but also with the change in work hardening rate which affects the deformation process in Charpy specimens. The models of trans-granular cracking showed by various workers due to formation of coarse carbides on tempering reduce the critical stress required for initiation of brittle crack.

## Experimental Procedures:

### 3.1 Material:

The material used in present investigations has following composition (very close to AISI 4125). Currently this has been used in chain links of earth moving equipments and other high strength applications.

C %	Mn %	Si %	(S + P) %	Cr %	Mo %
0.33-0.37	1.1-1.4	0.35 MAX	0.05 Max	0.3-0.5	0.15

Ingots of this material were first rolled to 4" X 4" billets and then forged. All the samples required were machined out from forged billets.

### 3.2 Preparation of Test Specimens:

#### a) Charpy V Notch Specimens:

Standard Charpy V notch samples were prepared according to following dimensions:

Length of sample = 58 mm

Area of cross section = 10 mm X 10 mm

Depth of V notch = 2 mm

Angle of notch = 45°

Notch root radius = 0.25 mm

The specimen is shown in the figure 3.2a

b)  $K_{IC}$  specimens:

Specimens for fracture toughness testing were prepared as per ASTM standards. Three point bend test was carried out to evaluate the fracture toughness. In order to find valid  $K_{IC}$  values, the necessary requirement of thickness of the sample which will produce plane strain condition is most important. This is being confirmed by following relation.

$$B \geq 2.5 \left( \frac{K_{IC}}{\sigma_{ys}} \right)^2$$

Where ,

$B$  - Thickness of specimen.

$K_{IC}$  - Estimated fracture toughness.

$\sigma_{ys}$  - Yield strength of material.

The specimen used in case of tempering temperature 200° C, 250° C, 300° C had following dimensions (small samples)

Thickness	$B$	16 mm
Width	$W$	32 mm
Total length	$L$	152 mm
Span	$S$	128 mm
Crack to width ratio $\frac{a}{W} = 0.45$ to 0.55.		

When it had been found that the fracture toughness test gave invalid results using above dimensions for 400° C, bigger specimens having thickness 1.5 times that of previous sample were used. According to this thickness other

dimensions also change and are as follows (big samples)

Thickness	B	24 mm
Width	W	48 mm
Total length L		200 mm
Span	S	192 mm

The crack length  $a$  include both the depth of notch and the length of fatigue crack. The fatigue crack starter notch was machined in the specimen before the heat treatment. The specimen is shown in the figure 3.2 b

### 3.3 Heat Treatment:

All the samples of Charpy V notch test & plane strain fracture toughness test were heat treated according to the following schedule :

Austenitisation temperature	:	870° C	1 $\frac{1}{2}$ hrs.
Quenching	:	in oil	( Room Temperature)
A) Tempering	:	for CVN test	
for 1 $\frac{1}{2}$ hrs.		200, 250, 300, 350, 400 ° C	
		For $K_{IC}$ test	
		200, 250, 300, 400 ,450, 500, 550°C	
B) Tempering at varying time	:	for 350 °C ( CVN test )	
		2 , 4 , 8 hrs	

After tempering all the samples were air cooled to room temperature.

All the heat treatments were carried out in muffle furnaces with electronic temperature controllers. Pt / Pt Rh and Chrome - Alumel thermo couples were used for temperature measurements. Cast iron filings were used to cover the samples for preventing or minimising decarburisation and oxidation of samples.

### 3.4 Mechanical Testing:

a) For impact toughness testing a pendulum type Charpy V-notch testing machine was used. Hammer velocity was 3.3 m/sec in accordance with ASTM standards.

b)  $K_{Ic}$  specimens were tested using a Material Testing System (MTS 810 model) machine of 10,000 kg capacity. The samples for fracture toughness testing were first subjected to fatigue precracking.  $\sigma_{min}/\sigma_{max}$  ratio was kept + 0.1 during fatigue precracking. If the load cycle is maintained constant, the maximum K (stress intensity) and the K range will increase with crack length. Higher K values result in undesirable high crack growth rates. Therefore both maximum and minimum loads were continuously decreased with crack length keeping  $\sigma_{min}/\sigma_{max}$  constant. The frequency used was 15 Hz. The testing and evaluation of fracture toughness values were carried out in accordance with the ASTM standard - E399. All the fracture toughness values were found to be valid  $K_{Ic}$  values using minimum specimen thickness criterion with different samples of different strength levels.

c) Hardness testing was done on a Rockwell Hardness Tester using C scale.

Large number of readings were taken on throughout the specimen and then

20/05/2020

### 3.5 Scanning Electron Microscopy:

In order to analyze the microstructures present in different tempering conditions (i.e. with varying time and temperature of tempering), use of SEM as metallographic tool was made. Also the fracture surface studies were made using the same microscope (JEOL SM 840).

**3.5 A) Metallography:** The samples needed for metallography were prepared from the Charpy and  $K_{Ic}$  specimens. In this case, specimens of different tempering conditions were cut parallel to the fracture surface. These were then rough polished on emery papers and then fine polished. The etchant used was 5% Nital solution. In order to reveal the true microstructure re-etching and repolishing was done. Etched samples were then observed under SEM. In case of quenched and tempered steels, the microstructural features cannot be revealed under optical microscope. Microstructural studies under SEM were done using two types of signals -

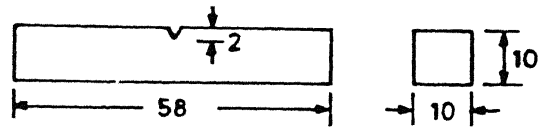
- 1) Secondary electron signals (S.E.)
- 2) Backscattered electron signals (B.E.)

From both S.E. signals come from the shallow regions of etched samples and were due to the etching difference of phases present in the samples. The B.E. signals are produced according to compositional difference in adjacent areas and they come from deeper regions of sample. It was noted that the image produced by B.E. signals was not sharp and was rather weak. The images produced by S.E. signals were satisfactory. It was confirmed that the microstructures obtained in two different modes of signals were one and the same. In this way the elimination of

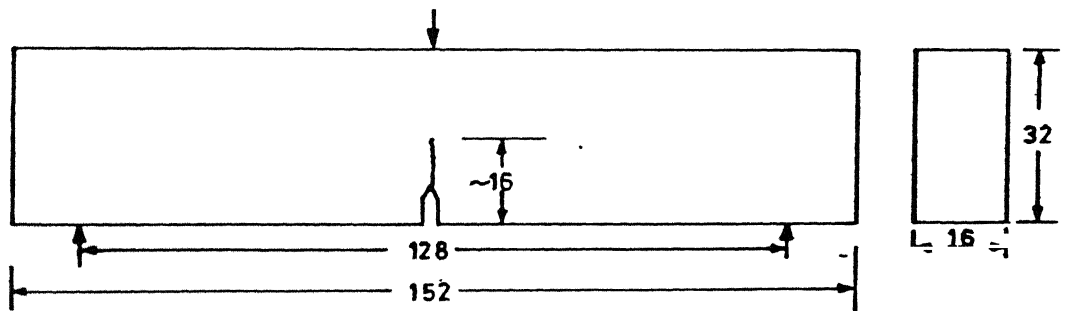
any etching faults was possible, which otherwise would have interfered with the microstructural features. The accelerating voltage used was 20 kV for both metallographic and fractographic studies.

3.5 B) Fractography : The fractured samples from CVN test and fracture toughness test were cut to analyze fracture modes present in different tempering conditions. In this study also, the SE mode has been used with different levels of magnifications.





(a) Charpy V notch specimen



(b)  $K_{IC}$  Specimen (three point bend)

(All dimensions are in mm)

Fig. 3.1

## Experimental Results and Observations:

---

The experimental results obtained in the present investigation for the given steel are reported as follows:

### 4.1 Variation of Hardness with Tempering Temperature:

Hardness values of the steel used in this investigation for various treatments are given in the following Table 4.1. The values reported are the average of a large number of readings taken for each treatment.

Table 4.1

Tempering Temperature (°C)	As quenched	200	250	300	350	400	450
Hardness (RC)	55	50	48	45.5	45.0	40.5	38.0

Figure 4.1 show the hardness variation with tempering temperature. The hardness decreases with increasing tempering temperature. The decrease in values are more rapid after 250° C.

### 4.2 Charpy Impact Toughness Variation:

The Charpy V-notch impact toughness values for various tempering temperature are shown in following table 4.2. These are based on average of three

specimens tested

Table 4.2

Tempering Temperature ( $^{\circ}$ C)	Impact Energy (J)
As Quenched	22.5
200	106.8
250	61.7
300	48.5
350	11.76
400	29.4
450	69.6

Figure 4.2 shows variation of impact toughness with tempering temperature. From as quenched condition the impact values increase up to  $200^{\circ}$  C and after that it starts decreasing up to a value less than as quenched specimen at  $350^{\circ}$  C. The values are again increasing above  $350^{\circ}$  C. This is the classical T.M.E. trough obtained in this type of steel.

#### 4.3 Plane Strain Fracture Toughness ( $K_{IC}$ ) Variation:

The result of plane strain fracture toughness testing using three point bend test are shown in following table 4.3.

Table 4.3

Tempering Temperature (°C)	Fracture Toughness (MPa $\sqrt{m}$ )
300	53.5
350	82.0
380	115
400	82.0
450	33.03
500	66.45
550	130.46

In case of plane strain fracture toughness using two different types of specimen sizes, according to requirement of valid  $K_{IC}$  in different tempering conditions, are tested. Figure 4.3 shows the occurrence of T.M.E. still in  $K_{IC}$  testing but there is shift of 100° C in the T.M.E. range as obtained in CVN test. This shift of T.M.E. has been observed only due to testing of tempered specimens in the whole range of temperature. The earlier results have been found only upto 400° C in which the possibility of T.M.E. at 450° C have been ignored. Thus the peak of T.M.E. trough in  $K_{IC}$  occurs at 400° C which is recovered temperature for CVN testing. The actual minimum values in the trough are around 450° C at which CVN values are of higher order. At 500 and 550° C the  $K_{IC}$  are again recovered. This variations have been reported in figure 4.3.

#### 4.4 Variation of CVN Values with Time at 350° C:

As it has been found that T.M.E. in CVN testing occurs at 350° C, tempering for various time has been performed and the CVN testing of those specimens was done. Temperature of tempering as well as time may change the kinetics of tempering transformations. This was the main intention of this study. The CVN

impact toughness values for various times at 350° C are shown in Table 4.4.

Table 4.4

Tempering Time (hours) at 350° C	Charpy Impact Toughness (Kg-m)
2	1.2
4	0.95
8	0.95

It is found that there has been no beneficial effect of longer tempering time at 350° C. The values are rather decreasing instead of increasing. This trend has been shown in Fig. 4.4.

★ In a small experiment Charpy Specimen before tempering at 350° C had been prestrained at 200° C to a very small strain. This also has not been useful in improving the impact values at 350° C (T.M.E.).

#### 4.5 Microstructural Study:

##### a) Variation of Tempering Temperature:

The microstructures obtained from the polished and etched samples of varying temper conditions under SEM are shown in Figs. 4.5.1, 4.5.2, 4.6.

The microstructure of quenched and temper steel consists mainly of lath martensites, very fine and having different size and orientations. The sample tempered at 200° C (plate 149) shows such features. The white portions obtained in

sample of 350° C (plate 111) tempering shows the carbide phase precipitated from the martensite laths. Also there has been some sort of widening of these laths with carbides forming at lath boundaries. The essential feature at this tempering temperature (350° C) is that the carbides are ribbon shaped of a film type morphology.

In an another micrograph of 400° C tempered sample (plate 107), it is observed that the ribbon shaped carbides start necking down. There has been start of spherodization with small white round carbides seen at some places. The process of spherodization continues and the amount of film like carbides lowers with still higher tempering temperature of 500° C (plate 219). At 550° C the microstructure predominantly consists of spherodized carbides and they coagulate to form bigger carbide portions (plate 220). The volume fraction of ferrite is also increasing at 350° C and higher temperature tempered condition. The carbide films that have formed at 350° C tempering are of the order of 0.6 to 0.8  $\mu\text{m}$  and some places they may be found to be as big as 1  $\mu\text{m}$ . Thus there has been clear change in microstructure from 200° C to 550° C. Initially present packet martensite first precipitates the carbides (which then coarsen) followed by spherodization. In each case the volume fraction of ferrite is increased.

#### **b.) Variation of Tempering Time:**

The microstructure of samples tempered longer time at 350° C are shown in Fig. 2. It is clear from those microstructures that no spherodization can be possible by longer tempering at 350° C. The features of ribbon shaped carbides are still present.

Fig 4.7 shows the schematic representation of morphological changes in carbides during tempering.

#### 4.6 Fracture Surface Studies:

The fracture surface of samples fractured under CVN testing and fracture toughness testing are shown in Figs 4.8.1, 4.8.2, 4.9.1 and 4.9.2.

##### a) CVN Fracture Surfaces:

The fracture mode predominantly existing in sample tempered at 200° C (plate 148 and plate 149) is quasi cleavage. Poorly ill-defined small cleavage facets are seen at some places. Features of river patterns at one place (right top) also can be seen. The poorly cleaved regions are surrounded by dimples of very fine nature.

Plate 97 and 96 shows domination of cleavage mode at 350° C tempering. At higher magnification this feature is predominantly seen. The amount of ductile dimple features is very small. The cleavage mode which is of interlath nature is confirmed by fractograph taken for longer time (8 hrs) tempered sample at 350° C (plate 151 and 13). The cleavage is more clearly seen at higher magnification.

In case of 400° C tempering mode of fracture again changes. The plates 105 and 104 shows it is predominantly tear rupture with lot of dimples.

##### b.) Fracture Surfaces of $K_{IC}$ samples :

The fractograph of sample tempered at 450° C (plate 87) shows partly rupture and partly cleavage. The domination of cleavage is not as much as is found in CVN samples at 350° C.

The 500° C tempered samples have failed more by tear rupture than by cleavage (plate 143 and 145). This trend of increasing tear rupture continues still at higher temperatures upto 550° C (plate 221, 224).

CENTRAL LIBRARY

109078

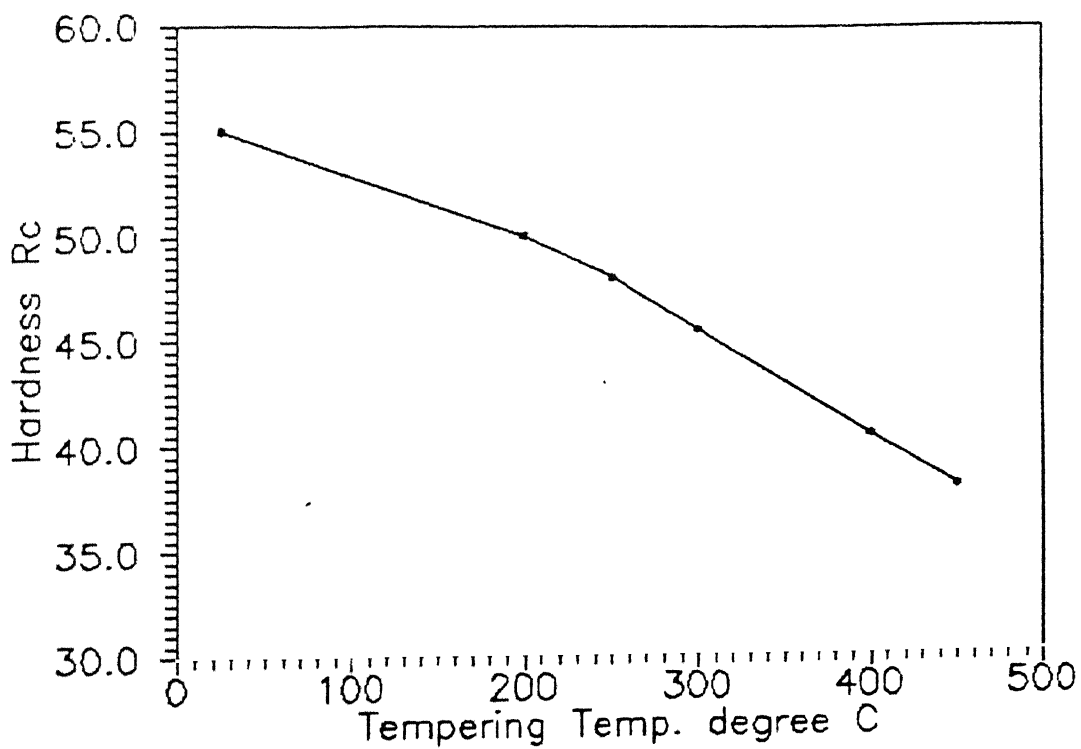


Fig4.1 Shows Variation of Hardness with Tempering temperature.



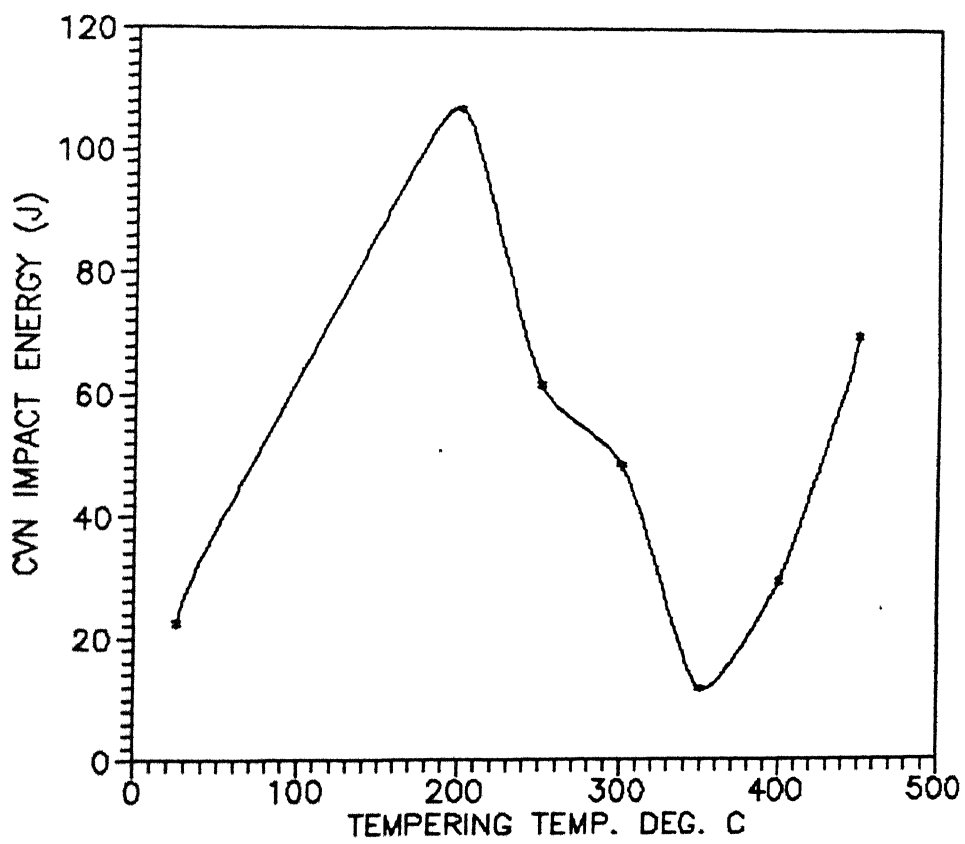


FIG. 4.2 SHOWS VARIATION OF CHARPY VALUES WITH TEMPERING TEMP.

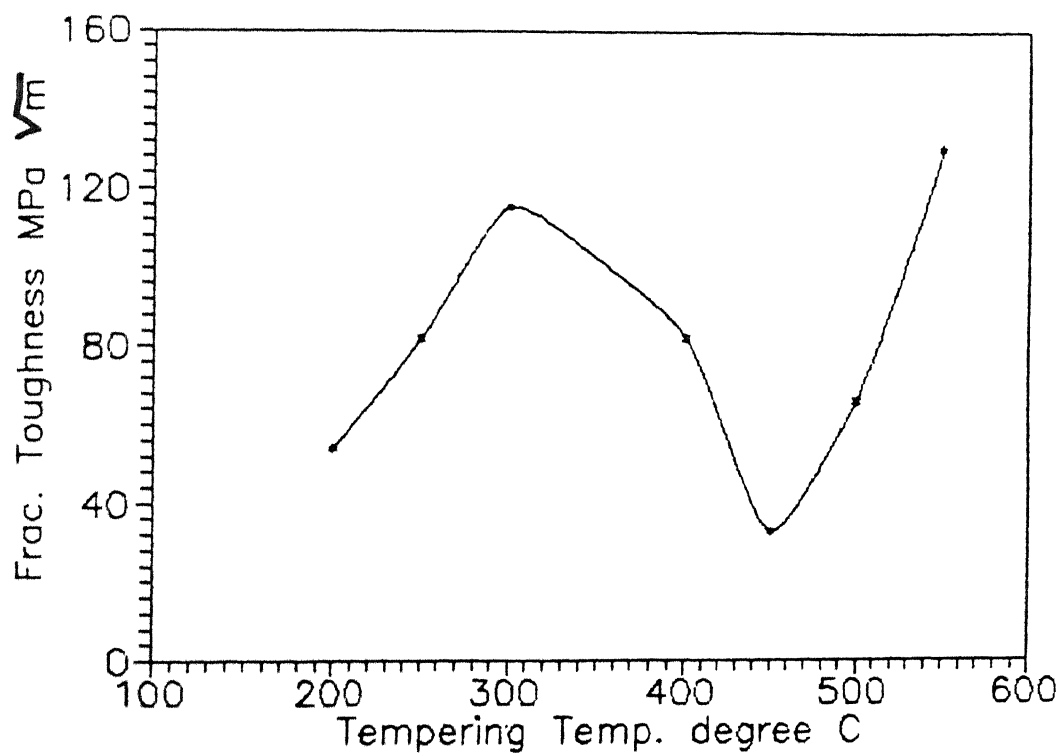


fig:4.3 Shows Fracture Toughness values with Tempering Temperature.

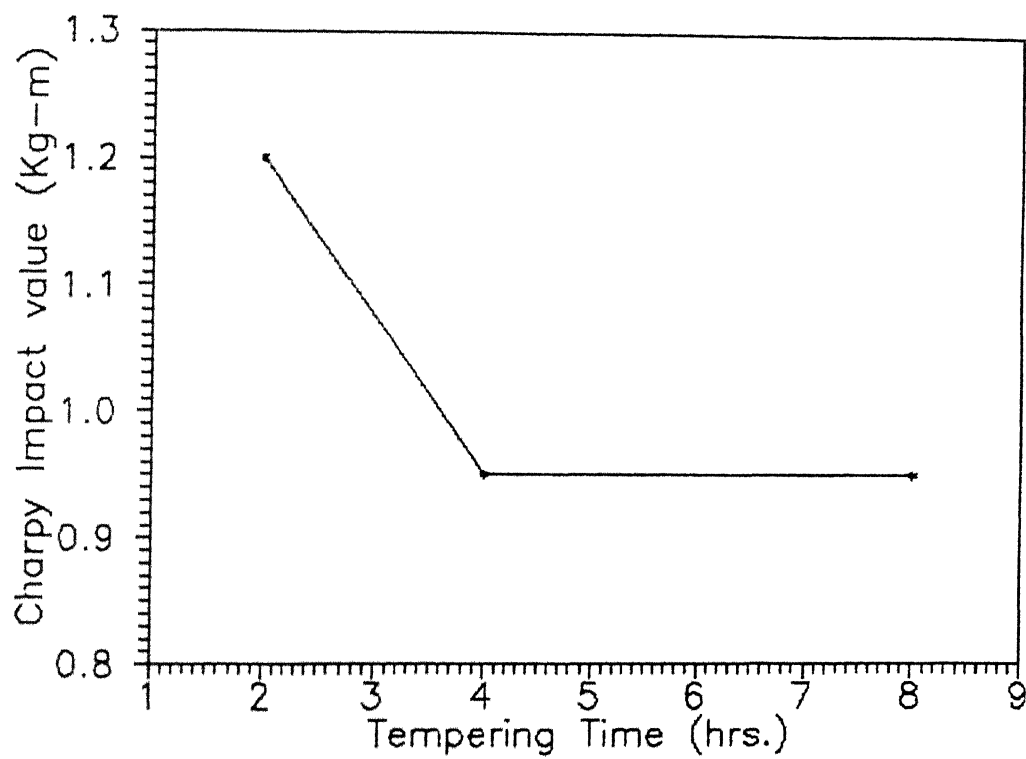
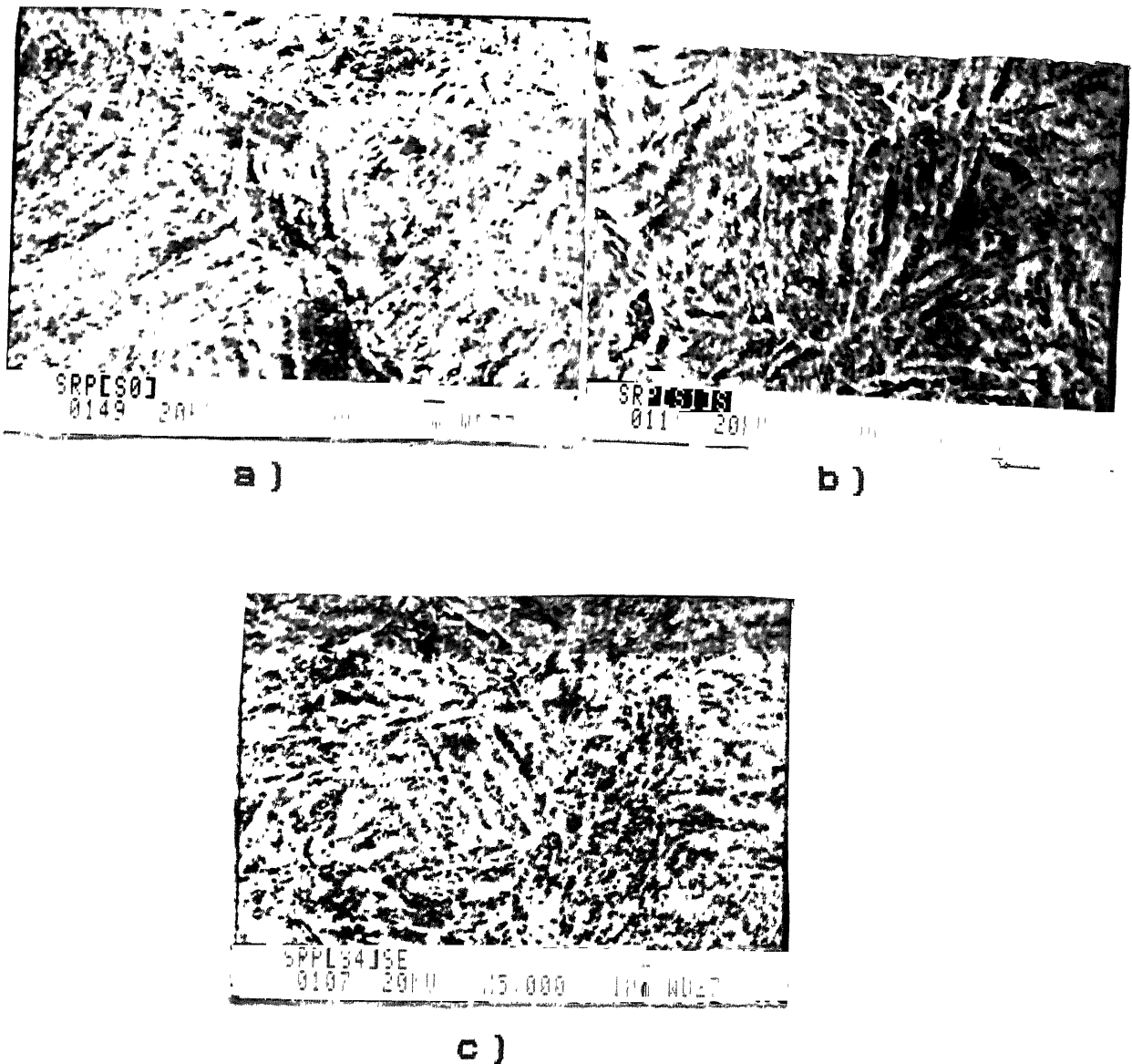


Fig 4.4 Shows variation of C V N values with varying tempering time at 350 degree Centigrade.

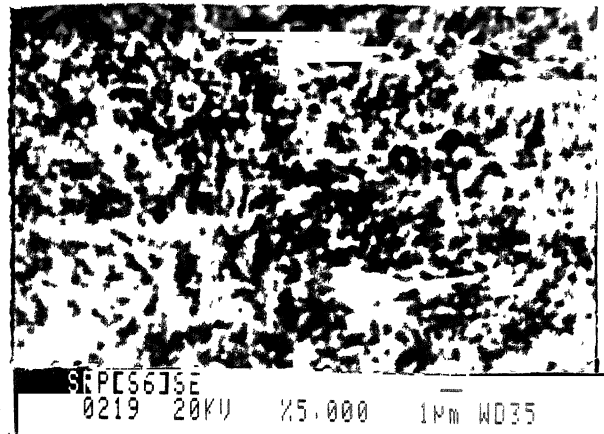


**Fig. 4.5 .1** S.E.M. Micrographs of specimens austenitised at 870° C for 90 min. oil quenched and tempered at a) 200° C , b) 350° C , c) 400° C

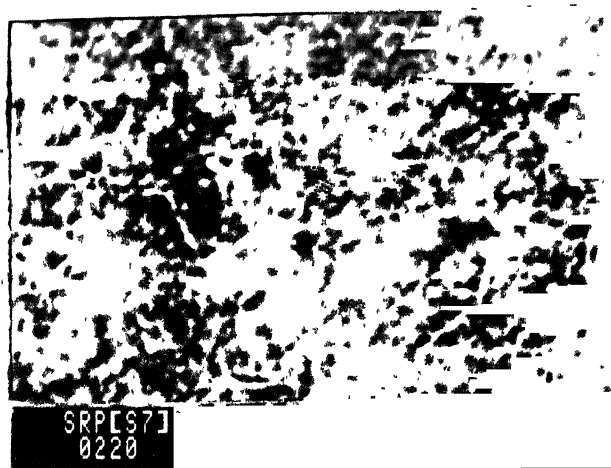
★ The respective magnification , Working Distance ( W.D. ) & Plate No. etc. are shown on each plate.



d )



e )



f )

**Fig. 4. 5. 2** S.E.M. Micrographs of specimens austenitised at 870° C for 90 min.  
oil quenched and tempered at d) 450° C , e) 500° C , f) 550° C

★ The respective magnification , Working Distance ( W.D. ) & Plate No. etc. are shown on each plate

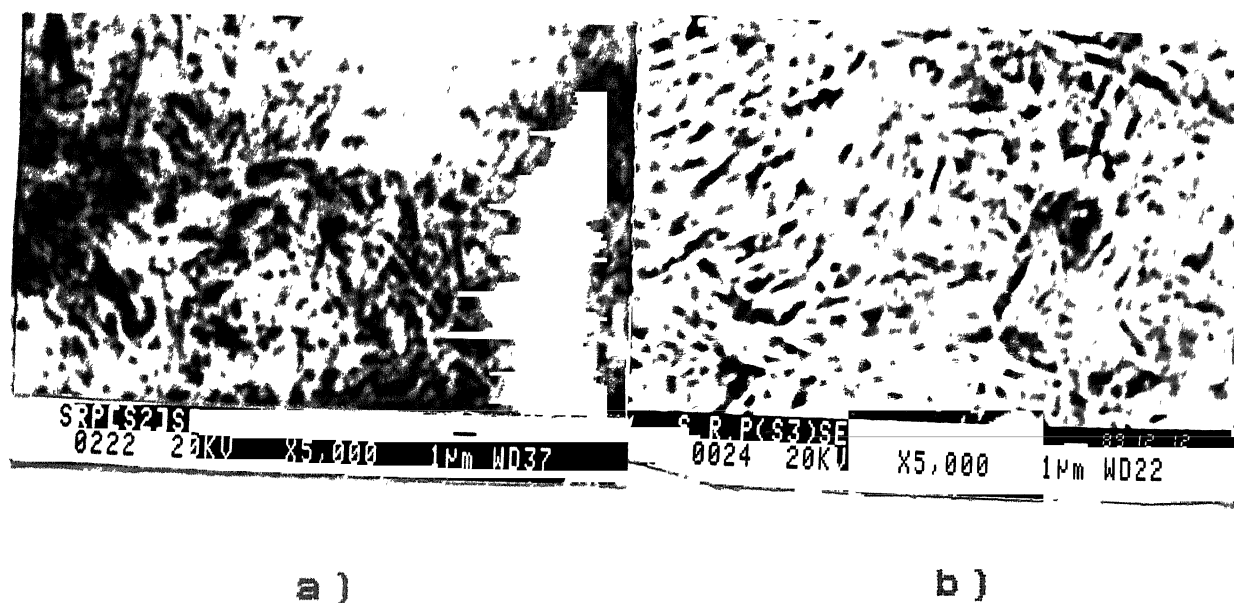
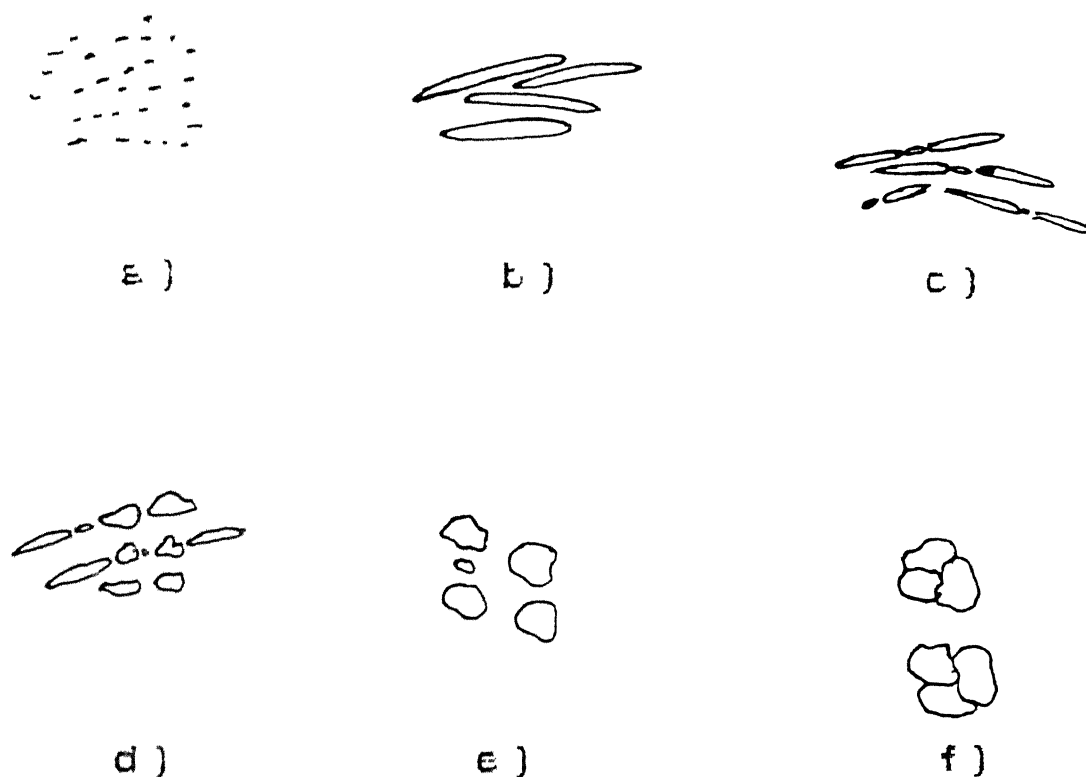


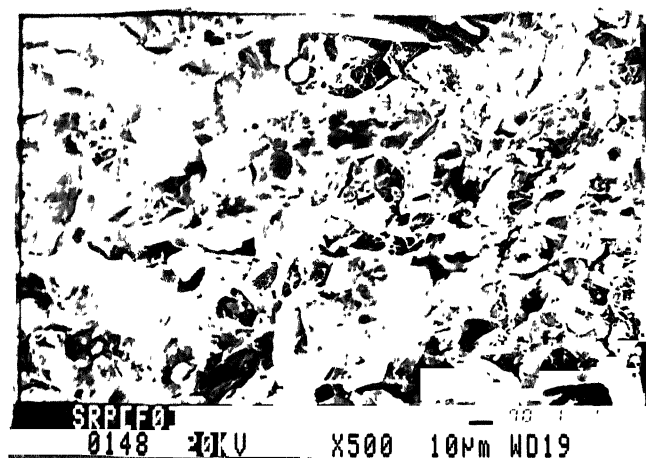
**Fig. 4. 6** S.E.M. micrographs of specimens austenitised at  $870^{\circ}\text{C}$  for 90 min. oil quenched and tempered at  $350^{\circ}\text{C}$  for a) 4 hrs. & b) 8 hrs.

★ The magnification, magnification, Working Distance ( W.D. ) & Plate No. etc. are shown on each plate.



- a)  $\epsilon$  - Carbide ( $200^{\circ}\text{C}$ ) , b) Ribbon shaped carbide ( $350^{\circ}\text{C}$ ),  
 c) Necking down of carbide ( $400^{\circ}\text{C}$ ) , d) Initiation of spheroidization  
 after necking ( $450^{\circ}\text{C}$ ) , e) Spheroidal carbide ( $500^{\circ}\text{C}$ ) ,  
 f) Coagulation of spheroidal carbide ( $550^{\circ}\text{C}$ ) .

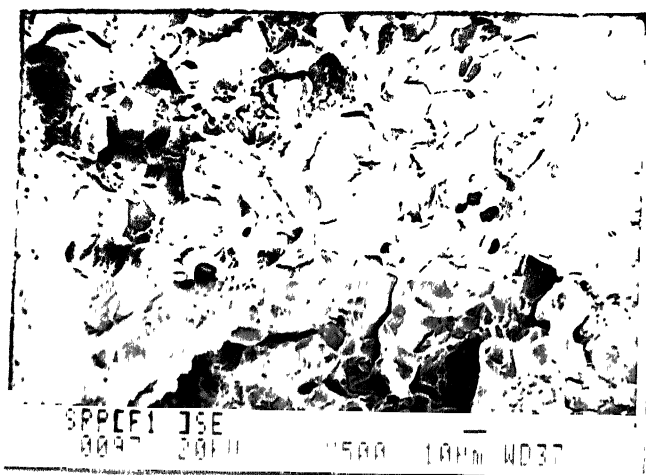
Fig. 4.7 Schematic representation of morphological changes taking place in carbide during tempering



a)



b)



c)



d)

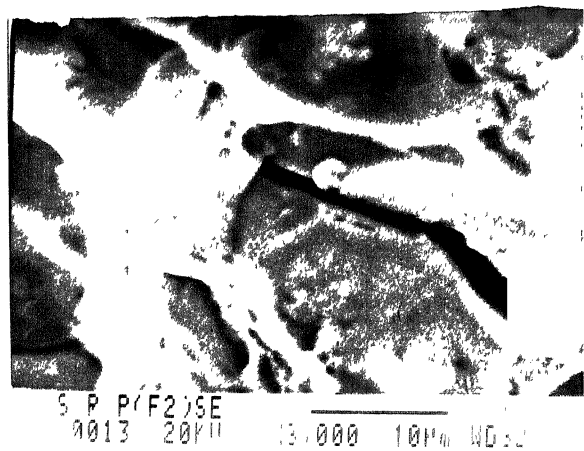
**Fig. 4. 8. 1** S.E.M. Fractographs of C V N specimens austenitised at 870° C for 90 min. oil quenched and tempered at a) & b) 200° C , c) & d) 350° C

★ The respective magnification , Working Distance ( W.D. ) & Plate No. etc. are shown on each plate.

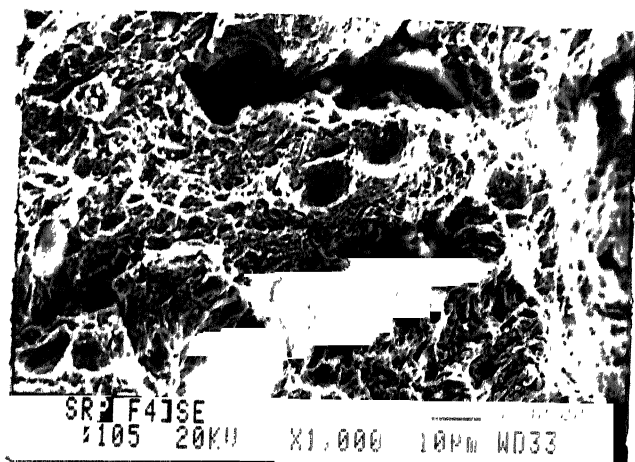




e)



f)



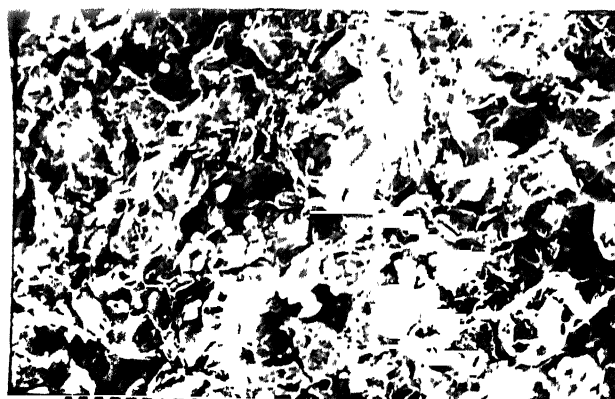
g)



h)

**Fig. 4. 8. 2** S.E.M. fractographs of C V N specimens austenitised at 870° C for 90 min. oil quenched and tempered at e) & f) 350° C ( 4 hrs. )  
g) & h) 400 °C

★ The respective magnification , Working Distance ( W.D. ) & Plate No. etc. are shown on each plate.



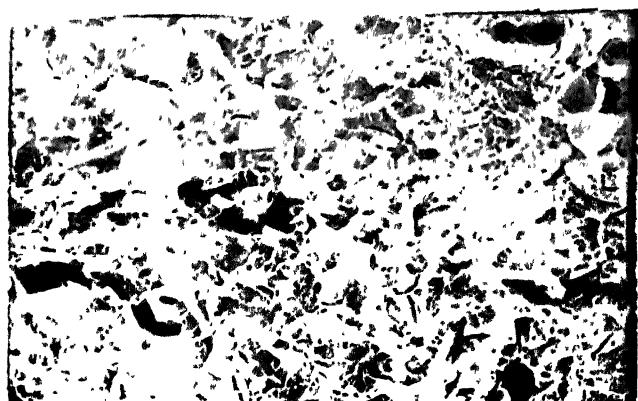
SRP[FT1]SE  
0087 20KV X500 10µm WD39

a)



SRP[FT1]SE  
0086 20KV X2,000 10µm WD39

b)



SRP[FT2]  
0145 20KV X500 10µm WD22

c)

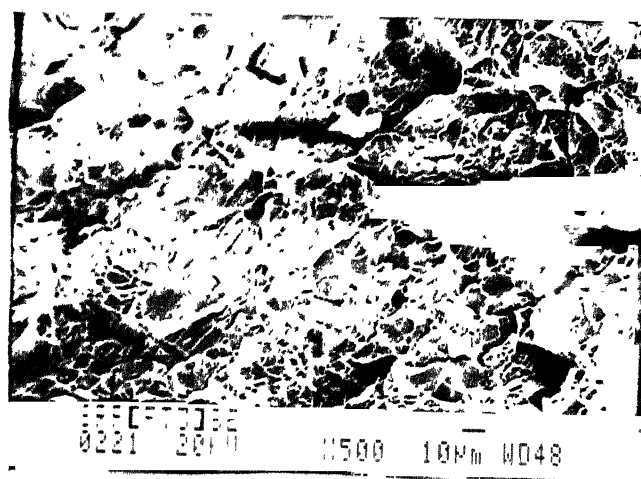


SRP[FT2]  
0143 20KV X2,000 10µm WD22

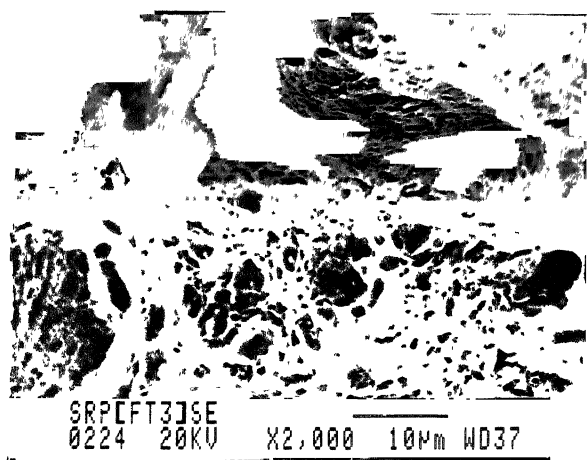
d)

**Fig. 4.9.1** S.E.M. Fractographs of  $K_{IC}$  specimens austenitised at  $870^{\circ}\text{C}$  for 90 min. oil quenched and tempered at a) & b)  $450^{\circ}\text{C}$ , c) & d)  $500^{\circ}\text{C}$

★ The respective magnification, Working Distance (W.D.) & Plate No. etc. are shown on each plate.



e)



f)

**Fig. 4. 9. 2** S.E.M. Fractographs of  $K_{ID}$  specimens austenitised at  $870^{\circ}\text{C}$  for 90 min. oil quenched and tempered at  $550^{\circ}\text{C}$ .

★ The respective magnification , Working Distance ( W.D. ) & Plate No. etc. are shown on each plate.

## Discussion:

---

In earlier sections, results of present investigations were presented. Results show the presence of Tempered martensite Embrittlement in both the evaluation methods used for toughness measurements. The occurrence of T.M.E. in Charpy impact testing is observed in the same range of tempering temperature as was observed in many earlier references in 4340 and 4140 type steels. The most interesting feature of present study points out the shift of the T.M.E. range in  $K_{IC}$  testing. In some references the T.M.E. was assumed to be absent for  $K_{IC}$  testing in which the testing of samples were restricted only upto 400° C. In one study by Lee et al<sup>53</sup> showed the occurrence of T.M.E. in  $K_{IC}$  testing but was in the same range as that had been observed for Charpy Impact Testing. When the entire range of tempering temperature had been tested in present investigations, shift of T.M.E. by 100° C from Charpy T.M.E. range was found. As the shift of T.M.E. temperature range due to change in evaluation methodology was found it became necessary to analyze the two T.M.E. phenomenon in different manners. It is also important to resolve the mechanisms involved in two different embrittlements.

### The T.M.E. phenomena in Charpy Test:

In order to make the study more simple the T.M.E. trough obtained in Charpy Test can be considered to have three regions

- 1) Pre T.M.E. region
- 2) Actual T.M.E. region
- 3) Post T.M.E. region

### 1) Pre-T.M.E. Region (Charpy Test) (upto 200° C):

In this region the impact toughness values are increasing from as-quenched stage to 200° C tempering. At 200° C the T.M.E. trough has its peak value. The well established facts of strain relieving of quenched martensitic structures and precipitation of  $\epsilon$  carbide at and around 200° C are the most probable reasons for improvements in toughness values. The observed fracture mode in this range is of quasi-cleavage type, which is less brittle. The microstructure consists mainly of packet martensite and  $\epsilon$  carbide which is not resolvable even at high magnification. Combining the microstructure and fracture mode observed in this pre-T.M.E. region, it is necessary to note that even though in presence of  $\epsilon$  carbide as a hard phase, there has been no drop in toughness values. This is predominantly due to very fine size and homogeneous distribution of hard phase throughout the structure.

It therefore implies that this morphology of even distribution of fine hard phase with no ferrite phase present at this low temperature causes to improve overall toughness level.

### 2) Actual T.M.E. Region:

In the temperature range from 200° C to 350° C, there has been a drastic drop in toughness values. The typical microstructure at 350° C consists of coarse cementite phase with ribbon (film like) shaped morphology. The fracture mode is fully dominated by the transgranular (interlath) cleavage facets. This observations of cleavage fracture also have been made in earlier references with 4340 and 4140 pure steels.

The mechanism for this type of brittle fracture may be the cleaving of coarse carbide phase in front of crack tip. The ferrite content at this tempering

temperature is also very less. As there has been no indication of cleavage in specimens at or below 200° C tempering, the presence of coarse and typical ribbon shaped morphology must be responsible for this type of embrittlement. Another fact in such mechanism of embrittlement also comes out is that the gradual coarsening of the ribbon shaped carbide with increasing tempering temperature is reproduced by equal drop in impact toughness values (i.e. drop in values between 200° C to 350° C).

The mechanism proposed by G. Thomas<sup>8</sup> is also applicable in the present study. It suggests that, as a result of intense slip interactions, immobile dislocations can be formed which eventually raise the stress locally to fracture level. The locations of such process are at carbide phase present at inter and intra lath regions. There is plastic flow restriction observed in those places which is created by the typical size, shape and distribution of carbides. In addition to this type of cleavage mechanism, many references pointed towards the impurity assisted intergranular mechanism. Such fracture modes have not been observed in present study and can be attributed to low level of impurity (S + P) content.

Thus main factor comes out of this discussion for Charpy T.M.E. is the size, shape and distribution of typical carbide phase and effect of this morphology on slip distribution and crack initiation.

### 3) Post T.M.E. Region:

The significant features of microstructure of specimens tempered in this region (400° C and above) is of spherodization of filmy carbide and increase in ferrite content. This is the main cause of ductile fracture mode observed. The impact toughness improvement is also found to increase with greater and greater

spherodization and ferrite content in structure. For this type of structure, cleavage crack nucleation will be more difficult due to high particle/matrix bond strength. Therefore it requires higher stress levels to break such bond. As the carbide morphology is spherical instead of cleavage of carbide phase, the shear band between stressed crack tip and carbide particles produces microvoids. Thus it produces ductile type fracture mode as observed in 400° C tempered specimen. The only reason of this ductile fracture with improvement in toughness value may be the spherodization effect.

Before making any arguments about T.M.E. in  $K_{IC}$  testing it is now necessary to distinguish the two evaluation methods. The conditions prevailing in these two different methods may have different interactions of crack tip with microstructure.

*The  $K_{IC}$  test and Charpy test differ in that each test has its own associated stress field in the fracture origination region, Strain rate and specimen dimensions requirements.*

In general the effect of strain rate is always represented by lowering of transition temperature for slower strain rates ( $K_{IC}$  testing). This aids in ductile behavior of same material at same state of microstructural conditions. In relatively narrow specimens, containing relatively blunt notches (Charpy V) the amount of plastic strain and hence the amount of strain hardening that occurs just in front of notch before general yielding is extremely small. Thus it seems that the Charpy method is more stress controlled and the decrease in Charpy energy can be attributed to decrease in fracture energy. Further more such a loss creates shift in transition temperature. The fracture initiation mechanisms found also supports this by producing stress assisted cleavage type fracture mode.

In case of  $K_{IC}$  testing, which is a strain controlled test, due to triaxiality of

specimen used, the fracture mode adopted is due to certain field (upto a certain range of distance) in front of crack tip. The necessary requirements of critical crack length  $a_0$  to grow catastrophically is also of higher order.

Thus after considering these basic differences involved in two different test conditions and also the fracture initiation process, it is easy to analyze TME in  $K_{IC}$  testing.

#### 1) Pre T.M.E. Region ( $K_{IC}$ Test):

In this test the  $K_{IC}$  values are increasing with tempering temperature upto  $400^\circ \text{C}$ . The mode of fracture in this region is also a ductile rupture. Although many microstructural changes occurred in this wide range, they didn't seem prone to strain controlled conditions and therefore didn't show any embrittlement. The probable reason for this may be, as stated by Lee et al<sup>53</sup>, that the inter carbide spacing has not reached to a critical level. In this region upto some temperature of tempering these cementite particles either are not big enough i.e in earlier stages upto  $(300^\circ \text{C})$  or if they do so coarsen, the inter particle spacing is not critical. This must have resulted in ductile rupture by void coalescence mechanism. As these carbides are major source of void formation, in this region the number of voids formed and the particle spacing is not producing any embrittlement. This is discussed in more detail in T.M.E. region analysis presented later.

Although in the same region where Charpy values are decreasing (mainly due to particular morphology of carbide failing by stress assisted cleaving), the  $K_{IC}$  values still keeps the trend of increase. This again suggests the non importance of shape of carbide phase in slower rate test ( $K_{IC}$  test).



### 2) Actual T.M.E. Region ( $K_{IC}$ Testing):

The temperature range from 400° C to 450° C, when the intercarbide spacing and number of voids produced between them are of critical level, the  $K_{IC}$  values are found to drop. Thus this drop at 450° C may be attributed to decrease in spacing of carbides. From microstructure, in this region the necking down of initial coarse ribbon shaped particle is being observed.

Similar considerations were made in fracture model proposed by Lee et al.<sup>13</sup> The model indicates the criterion of critical strain over a critical distance (i.e. the average spacing of cementite particles) to cause T.M.E.. During tempering in T.M.E. range a large number of cementite particles are precipitated and their dimensions are large enough to initiate the critical number of microvoids near the sharp crack tip.

Looking at the microstructure and the major fracture mode of low energy rupture plus some cleavage (mixed mode) at this T.M.E. range, above criterion of average inter particle spacing seems to fit for present case.

The cleavage facets observed, which may be probably due to local increase in yield strength of region in front of the crack, leads to cleavage at some places. The occurrence of this cleavage slightly hinders the proposed mechanism based on low energy rupture.

### 3) Post T.M.E. Region ( $K_{IC}$ Testing):

The tempering temperature at 500° C and above produces the microstructure of coagulated carbide particles. This process of coagulation decreases the number of carbide particles and increases the inter carbide particle spacing. The matrix at this temperature level is also soft ferrite in large amounts. These two facts

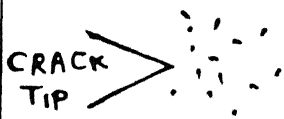
avoids the low energy tear rupture. The fracture mode observed is of ductile rupture and the proportion of this increases with increasing temperature

The proposed mechanism for present steel in Charpy and  $K_{IC}$  testing has been shown schemetically in Fig 5.1

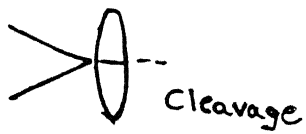
#### Variation of Time and Prestraining Effect:

The results obtained by prolong tempering at 350° C shows no improvement in the Charpy impact values. This may be due to the fact that time of tempering has little (negligible) effect on kinetics of tempering transformation. There has been no change in ribbon shaped morphology by prolonged tempering. But to support above mechanism of particular morphology of carbide phase, these results are also important.

Prestraining before T.M.E. range at 200° C to change the critical morphology prevailing at T.M.E. didn't produced any dramatic improvements and the values obtained were of same the order as that without prestraining



a ) Pre T. M. E



b ) T. M. E



c) Post T. M. E

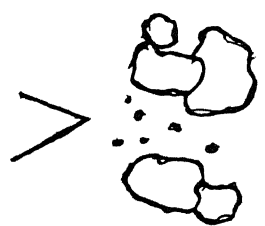
★ Stress assisted Cleavage fracture in T. M. E. region showing dependency of carbide morphology in C V N test



a ) Pre T. M. E.



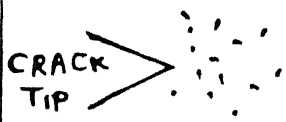
b ) T. M. E.



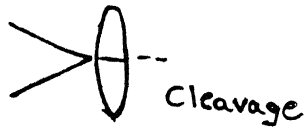
c) Post T. M. E.

★ Strain controlled Low Energy Rupture in T. M. E. of  $K_{IC}$  test due to critical inter-particle spacing & enough number of micro voids produced . No effect of carbide morphology in this test.

**Fig. 5-1** Schematic representation of Mechanisms proposed in C V N &  $K_{IC}$  testing in present steel.



a ) Pre T M E



b ) T M E



c) Post T M E

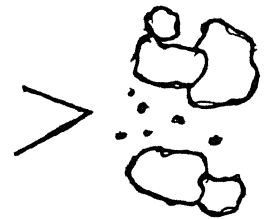
★ Stress assisted Cleavage fracture in T M E region showing dependency of carbide morphology in C V N test



a ) Pre T. M. E.



b ) T. M. E.



c) Post T. M. E.

★ Strain controlled Low Energy Rupture in T. M. E. of  $K_{IC}$  test due to critical inter-particle spacing & enough number of micro voids produced . No effect of carbide morphology in this test.

**Fig. 5-1** Schematic representation of Mechanisms proposed in C V N &  $K_{IC}$

testing in present steel.

---

**Conclusions :**

---

About Tempered Martensite Embrittlement phenomena in present steel (AISI 4135) , following conluding remarks can be made

- i ) Tempered Martensite Embrittlement was indicated by a trough in Charpy V-notch impact energy and  $K_{IC}$  plots
- ii) The range of tempering temperature over which the  $K_{IC}$  trough occurs, has been found to be shifted about 100° C higher than that of Charpy impact test (Charpy minima at 350° C and  $K_{IC}$  minima at 450° C was observed.)
- iii)The Charpy energy trough was found to coincide with the occurance of coarse ribbon shaped morphology of carbide resulting in cleavage at 350° C (T.M.E.). Thus the morphology of carbide was found to be the controlling factor in T.M.E. for this stress assisted Charpy test.
- iv)There has been no beneficial effects on T.M.E. of tempering for longer times. This shows time has no significance in improving the energy loss in the T.M.E. range.
- v)Since the fracture of  $K_{IC}$  specimens was primarily due to the ductile microvoid coalescence near the sharp crack tip, the spacing of cementite particles precipitated during tempering treatment was most important factor for interpreting the T.M.E results of plane strain fracture toughness.

Thus the study on effect of evaluation methodology on T.M.E. has been found useful in understanding the basic causes behind the interesting phenomena. Different mechanism of T.M.E are operating in two different evaluation methods (Charpy and  $K_{IC}$  test) due to the inherent characteristics of stress controlled or strain controlled fracture initiation process in each case. The practical implication of present investigation are

- ★ It is more dangerous to temper the steel components of this steel (AISI 4135) around 450°C as  $K_{IC}$  test is more compatible for material designing.
- ★ Tempering at 400°C is more safer in both respect, impact & static loading.

## References.

- 1.) G. Thomas: *Iron Steel*, 1973, vol 46, p 451
- 2.) G. Thomas: *Met Trans*, 1978, vol 9A, p.439
- 3.) J. McMohan & G. Thomas *Proc. International Conference on The Microstructure and Design of alloys*, Cambridge, vol.1, p. 180, Instt. of Metals, London. 1973
- 4.) D. Webster: *Met Trans*, 1971, vol. 2, p. 2097
- 5.) R.A. Clark and G. Thomas, *Met Trans A*, 1975, vol 6, p. 969
- 6.) E.C. Bain and H.W. Packston, *Alloying Elements in Steels*, second edition, American Society for Metals, Metals Park, 1966
- 7.) G.Y. Lai, W.E. Wood, R.A. Clark *Met Trans*, 1974, vol 5, p.1663
- 8.) M. Sarikaya, A.K. Jhinghan, G. Thomas, *Met Trans*, 1983, vol 14a, p. 1121
- 9.) H.K.D.H. Bhadeshia and D.V. Edmonds, *Metal Science*, June 1979, p. 325
- 10.) Jin Yu and C.J. McMohan Jr., *Metall Trans, A*, 1980, vol 11a, p. 291
- 11.) J.C. Murza and C.J. McMohan jr., *Trans ASME, J. Engg Metals and Tech*, 1980, vol 102, p. 369
- 12.) R.M. Horn and R. D. Ritchie, *Metall. Trans*, vol. 9A, Aug 1978, p. 1039
- 13.) H. Kwon and C.H. Kim: *Metall. Trans*, 1984, vol. 15A, p. 393
- 14.) H. Kwon and C.H. Kim: *Metall. Trans*, 1983, vol. 14A, p. 1389
- 15.) H. Kwon and C.H. Kim: *Metall. Trans*, 1986, vol. 17A, p. 745
- 16.) H. Kwon and C.H. Kim: *Metall. Trans*, 1986, vol 17A, p. 1173
- 17.) K.S. Lee: H. Kwon, Y.C. Lee, J.H. Lee and N.D. Cho: *J. Mater. So.*, 1987, vol. 22, p.4215
- 18.) Kwon, J.C. Cha and C.H. Kim: *J. Mater. So.*, 1988, vol. 100, p. 121
- 19.) Kwon and C.H. Kim: *J. Mater. So.*, 1983, vol. 18, p. 3671
- 20.) E.B. Kula and A.A. Anotil: *J Mater.*, 1964, vol. 4, p. 817
- 21.) J.M. Capus and G. Mayer: *Metallurgia*, 1960, vol. 62, p. 133
- 22.) J.R. Rellick and C.J. McMohan, *Metall. Trans*, 1974, vol. 5, p. 2439
- 23.) S.K. Banerji, C.J. McMohan, H.C. Feng, *Metall. Trans A*, 1978, vol. 9A, p. 237
- 24.) C.L. Briant and S.K. Banerji, *Metall. Trans*, 1979, vol. 10A, p. 1729
- 25.) C.L. Briant and S.K. Banerji, *Metall. Trans*, 1981, vol. 12A, p. 309
- 26.) C.L. Briant and S.K. Banerji and A.M. Ritter, *Metall. Trans*, 1982, vol. 13A, p. 1939
- 27.) J.E. King, R.F. Smith and J.F. Knott: *Proc. 4<sup>th</sup> Int. Conf. on Fracture*, Waterloo, D.M.R. Taplin, ed., 1977, vol. 2, p. 279
- 28.) J.P. Materkowski and G. Krauss: *Metall. Trans*, 1979, vol 10A, p. 1643

- 29.) J.R. Rellick , C.J. McMohan, H.C. Feng: Metall. Trans, 1978, vol. 9A, p. 237
- 30.) J.A. McMohan and G. Thomas. Proc. of International Conf. on Microstructure and Design of Alloys, Instt. of Metals, London, 1973, vol. 1, p. 180
- 31.) P. Bowen, C.A. Happsley and J.F. Knott: Acta Metall, 1984, vol. 32, p. 637
- 32.) Hoon Kwon and Chong Hee Kim, Metall. Trans, 1979, vol. 17A, p. 745
- 33.) E.P. Klier and A.R. Troiano: Metals Tech, 1945, vol. 12, p. 1
- 34.) P.M. Kelly and Nutting J. Iron Steel Instt., 1961, vol. 197, p. 199
- 35.) B. Edmonds and T. Ko: Acta Met. 1954, vol. 2, p. 235
- 36.) R.L. Rickett and J.M. Hodge: Proc. ASTM, 1951, vol. 51, p. 931
- 37.) C.W. Marschall, R.F. Hehemann and A.R. Troiano, Trans ASM, 1962, vol. 55, p. 135
- 38.) D.H. Huang and G. Thomas: Metall. Trans, 1971, vol. 2, p. 3433
- 39.) N. Bandyopadhyay and C.J. McMohan Metall. Trans, 1983, vol. 14A, p. 1313
- 40.) M.A. Grossmann, Trans AIME, 1946, vol. 167, p. 39
- 41.) L.J. Klingler, W.J. Barnett, R.P. Frohberg and A.R. Troiano: Trans ASM, 1954, vol. 46, p. 1557
- 42.) A. Nakashima and J.F. Libsch: Trans. ASM, 1961, vol. 53, p. 753
- 43.) C.L. Briant: Material Science and Technology, 1989, vol 5, p. 138
- 44.) D.A. Curry and P.L. Pratt, Material Science and Engineering, 1979, vol. 37, p. 223
- 45.) C.J. McMohan and M. Cohen, Acta. Metall., 1965, vol. 13, p. 591
- 46.) T.B. Cox and J.R. Low: Metall. Trans, 1974, vol. 5, p. 1457
- 47.) K.H. Schwalbe and W. Backfisch, Proc. 4<sup>th</sup> Int. Conf. on Fracture, Waterloo, D.M.R. Taplin, ed., 1977, vol. 2, p. 73
- 48.) V.H. Lindborg and B.L. Averbach: Acta. Met , 1966, vol. 14, p. 1583
- 49.) E.F. Walker and M.J. May: Frac. Tough. of High Strength Materials: Theory and practice : Iron and Steel Instt. Pub. 120, 1979, p. 135
- 50.) T.E. Swarr and G. Krauss, Metall. Trans, 1976, vol. 9A, p. 41
- 51.) R. Godse, G. Ravichandran and R.J. Clifton: Material Sc. Engg., 1989, vol. A 112, p. 79
- 52.) Y.C. Chi, S. Lee, K. Cho and J. Duffy: Material Sc. Engg., 1989, vol. A 112, p. 105
- 53.) S. Lee, D.Y. Lee and R.J. Asaro: Metall. Trans, 1989, vol. 20A, p. 1089
- 54.) E.J. Ripling: Trans. ASM, 1950, vol. 42, p. 439
- 55.) R.L. Rickett and J.M. Hodge: Trans. ASTM, 1951, vol. 51, p. 931
- 56.) C.L. Briant and S.K. Banerji, Metall. Trans, 1979, vol. 10A, p. 1151
- 57.) M.A. Grossmann: Trans. A.I.M.M.P.E., 1946, vol. 167, p. 39
- 58.) B.S. Lement, B.L. Averbach, M. Cohen: Trans. ASM, 1954, vol. 46, p. 851



- 59) A.A. Allten and P. Payson: Trans. ASM, 1953, vol. 45, p. 498
- 60) C.H. Shih, B.L. Averbach, M. Cohen: Trans. ASM, 1956, vol. 48, p. 86
- 61) C.J. Altstetter, B.L. Averbach, M. Cohen: Trans. ASM, 1962, vol. 55, p. 287
- 62) E.B. Kula, J.M. Dhosi: Trans. ASM, 1960, vol. 52, p. 321
- 63) J.M. Capus: J. of Iron and Steel Instt., 1963, vol. 201, p. 53
- 64) J. Baker, F.J. Lauter and R.P. Wie: ASTM STP 370, 1963, p. 3
- 65) B.R. Banerjee: ASTM STP 370, 1963, p. 94
- 66) B.R. Banerjee: J. of Iron and Steel Instt., 1965, vol. 203, p. 166
- 67) J.H. Bucher, G.W. Powell, J.W. Spretnak: Application of Fracture Toughness Parameters to Structural Material, H.D. Greenberg, ed. Gordon and Breach, N.Y., 1966, p. 323
- 68) C.N. Sastry and W.E. Wood: Material Science and Engg., 1980, vol No 45, p. 227
- 69) F. Zia-Ebrahimi and G. Krauss: Met. Trans.:1983, vol 14a, p. 1109.

ME-1990-M-PCN-TEN

108078

A 109078